Attribution Analysis of the Ethiopian Drought of 2015

SJOUKJE PHILIP,[a] SARAH F. KEW,[a] GEERT JAN VAN OLDENBORGH,[a] FRIEDERIKE OTTO,[b] SARAH O'KEEFE,[b] KARSTEN HAUSTEIN,[b] ANDREW KING,[c] ABIY ZEGEYE,[d] ZEWDU ESHETU,[d] KINFE HAILEMARIAM,[e] ROOP SINGH,[f] EDDIE JJEMBA,[f] CHRIS FUNK,[g] AND HEIDI CULLEN[h]

[a] *Royal Netherlands Meteorological Institute (KNMI), De Bilt, Netherlands*
[b] *Environmental Change Institute, University of Oxford, Oxford, United Kingdom*
[c] *School of Earth Sciences and Australian Research Council Centre of Excellence for Climate System Science, University of Melbourne, Melbourne, Victoria, Australia*
[d] *Addis Ababa University, Addis Ababa, Ethiopia*
[e] *National Meteorology Agency, Addis Ababa, Ethiopia*
[f] *Red Cross Red Crescent Climate Centre, The Hague, Netherlands*
[g] *U.S. Geological Survey, and University of California, Santa Barbara, Santa Barbara, California*
[h] *Climate Central, Princeton, New Jersey*

(Manuscript received 25 April 2017, in final form 29 September 2017)

ABSTRACT

In northern and central Ethiopia, 2015 was a very dry year. Rainfall was only from one-half to three-quarters of the usual amount, with both the ''belg'' (February–May) and ''kiremt'' rains (June–September) affected. The timing of the rains that did fall was also erratic. Many crops failed, causing food shortages for many millions of people. The role of climate change in the probability of a drought like this is investigated, focusing on the large-scale precipitation deficit in February–September 2015 in northern and central Ethiopia. Using a gridded analysis that combines station data with satellite observations, it is estimated that the return period of this drought was more than 60 years (lower bound 95% confidence interval), with a most likely value of several hundred years. No trend is detected in the observations, but the large natural variability and short time series means large trends could go undetected in the observations. Two out of three large climate model ensembles that simulated rainfall reasonably well show no trend while the third shows an increased probability of drought. Taking the model spread into account the drought still cannot be clearly attributed to anthropogenic climate change, with the 95% confidence interval ranging from a probability decrease between preindustrial and today of a factor of 0.3 and an increase of a factor of 5 for a drought like this one or worse. A soil moisture dataset also shows a nonsignificant drying trend. According to ENSO correlations in the observations, the strong 2015 El Niño did increase the severity of the drought.

1. Introduction

Ethiopia has faced multiple seasons of failed or erratic rainfall leading to one of the most impactful droughts in recent history. Farmers and pastoralists waited for the ''belg'' rains that generally occur between February and May in central and eastern Ethiopia, but in 2015 the belg rains came a month late after a false start. Farmers in one district, Combolcha, who planted early in the season, did not receive enough rain during the subsequent weeks for their crop to grow. Others waited too long for consistent rainfall, which also resulted in failed harvests.

A rapidly intensifying El Niño event was declared in March 2015 (by NOAA and IRI; Singh et al. 2016). In Ethiopia, El Niño can lead to drier conditions mainly in northwestern regions, especially affecting the rainy season known as ''kiremt'' that occurs from June through September. In 2015, the kiremt season was delayed and the rains were erratic and below average. Normally, kiremt rains account for 50%–80% of Ethiopia's annual rainfall while the combination of belg and kiremt seasons together accounts for about 90% of the total. In 2015, from only one-half to three-quarters

Denotes content that is immediately available upon publication as open access.

Corresponding author: Sjoukje Philip, sjoukje.philip@knmi.nl

DOI: 10.1175/JCLI-D-17-0274.1

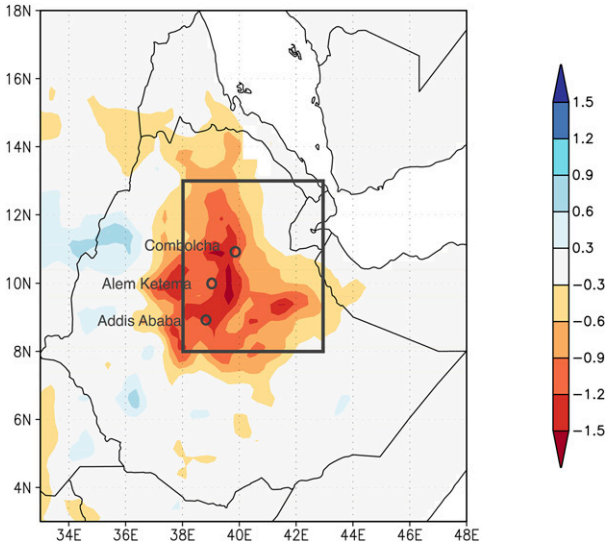

FIG. 1. Anomaly in precipitation (CHIRPS; precipitation minus 1981–2010 climatology) averaged over February–September 2015 (mm day^{-1}).

of the rainfall expected was received from February through September (Singh et al. 2016). Overall, 2015 was a very dry year in large parts of Ethiopia, as represented by rainfall anomalies from the Climate Hazards Group Infrared Precipitation with Stations (CHIRPS; Funk et al. 2015c) data (Fig. 1).

In December 2015, The government of Ethiopia and the United Nations (UN) jointly released a Humanitarian Response Document (HRD) calling for emergency assistance for 10.2 million people, in addition to 7.9 million people under the national social safety net program, the Productive Safety Net Programme (PSNP) (AKLDP 2016). Beyond total precipitation deficits, both the timing and the spatial distribution of rainfall impacted livelihood activities, such as agriculture and pastoralism (Singh et al. 2016). In 2016, many parts of central and northern Ethiopia were reported to be at least in crisis [Integrated Food Security Phase Classification (IPC), phase 3] food insecurity (FEWS NET 2017). The worst affected areas reported losses of over 75% of crop production and one million livestock, with a further 1.7 million livestock at risk because of poor body condition (IFRC 2017). By the end of 2016, projections showed that up to 22 million people required food relief assistance, with 1.7 million people estimated to experience from moderate to acute malnutrition (MAM) and 435 000 people estimated to experience from severe to acute malnutrition (SAM) (Government of Ethiopia and Humanitarian Partners 2016). The Government of Ethiopia and the international humanitarian community mobilized to meet emergency needs, including provision of water, sanitation and hygiene, and food and nutrition.

Naturally, questions that arise following such a disastrous event include asking to what extent the drought can be attributed to particular causes, whether another crisis like the one experienced in 2015 is likely to continue or worsen, and what can be done to better prepare for the next detrimental drought event. Many studies of the East African region have tried to address one or more of these issues but there are factors that make it far from straightforward to arrive at a unanimous conclusion. These include (i) slight differences in the research question and the framing thereof, (ii) the complex terrain and climatology of the area and Ethiopia's position in the dynamic global climate system that introduces large spatial and temporal variability in the rainy seasons, (iii) an unresolved paradox between observations and model results, and (iv) the challenge of achieving a clear, unbiased communication of the approach and results.

While no single study should claim to have the only answer, and each will have its own set of limitations, we take a number of steps toward managing the above factors, using "event attribution" to investigate the return periods and trends in Ethiopian droughts similar to the 2015 event. Event attribution is an emerging methodology that allows one to explore the extent to which human-induced climate change and possibly other factors are affecting localized extreme events (Stone and Allen 2005). Here we use a multimethod attribution approach, which implies that we fix the research question, or more specifically the event definition, but use a range of both models and observations and a combination of statistical and probabilistic methods to sample the method-related uncertainty, providing a measure of the confidence for the results. This method, which uses both observational and model analysis, has been used before in different types of attribution studies. For instance, attribution of droughts has been studied by Uhe et al. (2017, manuscript submitted to *Int. J. Climatol.*) and King et al. (2016); also, van der Wiel et al. (2017), Eden et al. (2016), and van Oldenborgh et al. (2016) [supplemented with a validation study by Philip et al. (2017, manuscript submitted to *Climate Dyn.*)] studied heavy precipitation events. Attribution studies for temperatures were carried out by, for instance, Sippel et al. (2016), Uhe et al. (2016), and van Oldenborgh et al. (2015). Considering the topographical and climatological complexity of Ethiopia, careful consideration is given to the spatial event definition. Using multiple models and model ensembles also partially samples the uncertainty due to modeled physics and the sensitivity to the representation of large-scale climate phenomena at the study location. We investigate the influence of climate change and El Niño–Southern Oscillation (ENSO)

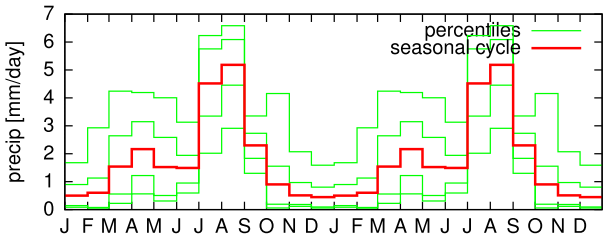

FIG. 2. Seasonal cycle of precipitation (red lines) in the study area in central–northeast Ethiopia (repeated over 2 cycles), showing the belg rains (February–May) and kiremt rains (June–September). The seasonal cycle is calculated over 1981–2010. Green lines show the 2.5th, 17th, 83rd and 97.5th percentiles. (Source: CenTrends data).

and comment on the magnitude of natural variability. To aid communication of the outcome, we also provide a (graphical) synthesis of the multimethod results, which is discussed in the context of our study's limitations.

The complexity of Ethiopia's topography and climate poses a challenge to those working to identify historical climatic trends and future projections. Ethiopia is a mix of low-lying semidesert mainly in the northeast and southeast and wetter highland mainly in the central and western regions. Seasonal precipitation patterns are highly variable, with some regions experiencing a single rainy season and others experiencing two or three wet periods within a given year. Much of Ethiopia experiences one main wet season (kiremt) from mid-June to mid-September. The northeastern, eastern, central, and southern highlands experience a secondary wet season (belg) characterized by sporadic and considerably lower rainfall accumulation from February to May. The belg forms the main rainy season for south and southeast Ethiopia, where a smaller third rainy season from October to November also occurs. The average seasonal cycle of central–northeast Ethiopia is shown in Fig. 2.

The kiremt season from mid-June to mid-September is influenced by the intertropical convergence zone (ITCZ) while traveling to its northernmost position and then retreating back toward the southwest. Other climate features influencing the kiremt rains include the tropical easterly jet (TEJ), the South Atlantic Ocean and southwest Indian Ocean anticyclone, and the East African low-level jet (EALLJ) (Endalew 2007). However, these relationships are very complex and many remain poorly understood (Segele and Lamb 2005) and in general do not give additional predictability. The global and regional climate drivers impacting the belg rain include the ITCZ, the subtropical westerly jet (SWJ) stream, the Arabian high, and the frequency of tropical cyclones over the southwest Indian Ocean (Endalew 2007; Diro et al. 2011a).

The impact of ENSO on Ethiopian rainfall has been well documented in the literature (Camberlin 1997; Degefu 1987; Diro et al. 2011b; Gissila et al. 2004; Korecha and Barnston 2007; Korecha and Sorteberg 2013; Segele and Lamb 2005). The warm phase of ENSO (El Niño) is associated with suppressed rains during the main wet season, kiremt, over northern and central Ethiopia; correlation coefficients with the Niño-3.4 index are $r \approx 0.5$ over these areas. Notably there is no strong connection to ENSO in the belg season, with regional differences present in the teleconnection sign.

From a global perspective, it would appear that Ethiopia, as part of central Africa, is at a location in the world where its mean climate and seasonal cycle are very well reproduced by climate models, when compared to other IPCC regions [see Figs. 9.38 and 9.39 of Flato et al. (2013) for the mean seasonal cycle and seasonal mean bias in temperature and precipitation]. The large-scale African monsoon system indeed stands out in its predictable response to worldwide SSTs (Hoerling et al. 2006). However, multimodel means over a wide area mask a lot of intermodel and regional variability, and the model's performance in reproducing climate extremes must be verified separately. Zooming in to subnational scales, we find that inconsistencies between reported results start to surface.

From a regional perspective, several observational studies indicate that Ethiopia is spatially and sometimes seasonally divided in its precipitation response to global warming. However, such studies are not in complete accord as to which regions or seasons are experiencing trends in precipitation. For example, on the annual time scale, drying trends are reported to be in the northwest (Jury and Funk 2013; data years 1948–2006), in southern regions (Viste et al. 2013; data years 1960–2002), or in no regions (Cheung et al. 2008; data years 1960–2002). On a subannual time scale, drying trends are reported for the southwest region but only during kiremt (Cheung et al. 2008; data years 1960–2002), for western regions during belg (Williams and Funk 2011), and for southern regions during both belg and kiremt (Viste et al. 2013; data years 1960–2002).

Viste et al. (2013) offer some insight into the disparity, noting that the lack of trend for northern regions is in accordance with studies using observations ending in 2002 or 2003, but that some other studies that include the more recent cluster of dry springs show a drying trend—a hint that conclusions on trends based on observational datasets are sensitive to variability within their limited length. The region in general also suffers from restricted public data access as well as incomplete gauge records, which can introduce large errors in data interpolation, especially where the complex terrain strongly impacts

the spatial distribution of rainfall. The above studies have at least one thing in common: the region that experienced extreme dryness in 2015 (northeastern Ethiopia) is not noted to be subject to a drying trend.

It is well known that there is an apparent disparity between observations and (projected) model results for the larger East Africa region, sometimes referred to as the East Africa climate paradox. A number of observational studies indicate a drying trend for the belg or "long rain" season over the past decades (Funk et al. 2005; Williams and Funk 2011; Lyon and DeWitt 2012; Viste et al. 2013; Liebmann et al. 2014), supported by the recent cluster of severe droughts, while most climate model projections indicate an increase in precipitation in a warming world (IPCC AR4; Shongwe et al. 2011; however, the evidence is less convincing in IPCC AR5).

To explain this apparent discrepancy, several hypotheses have been invoked (Rowell et al. 2015). These include (i) the quality of observational data being too poor (but this is rejected because of good evidence for an observed decline in recent decades), (ii) climate model trends being influenced by the inability of the models to reliably represent key physical processes (considered important for further investigation), (iii) natural variability being responsible for both past and future trends (considered unlikely as the only driver), and (iv) possibly genuine reasons for the contrasting trends, such as changing anthropogenic aerosol emissions (considered important for further investigation). Concerning (ii), we remark that, while unable to reject the hypothesis, Rowell et al. (2015) could also not find very strong evidence supporting it.

The attribution methodology offers a means to assess the influence of large-scale climate forcing or phenomena on the magnitude or probability of occurrence of a particular class of events of interest. There are only a handful of attribution studies for (East) Africa until the present, partly because of the limiting impact of short observational records (Marthews et al. 2015).

Funk et al. (2016) examined the 2015 Ethiopian drought, using similar methods to Funk et al. (2015b), and suggested that high Niño-3.4 temperatures, which they refer to as anthropogenically enhanced Niño-3.4 temperatures, may have increased the severity of the 2015 moisture deficits in northern Ethiopia. Their analysis only focused on the 2015 event, and the examined ENSO mechanism cannot account for long-term declines in Ethiopian rainfall. Their analysis suggested that recent high Niño-3.4 values may be higher than previous extremes, contributing to drier conditions in Ethiopia when there is a strong El Niño event. Purely dynamical indices of the strength of El Niño such as the Southern Oscillation index (SOI) and projections on GPCC land precipitation teleconnections, however, show no trend toward stronger El Niño events, either in the mean or in the strongest events (these indices also show the 2015/16 event to be weaker dynamically than 1982/83 and 1997/98). The trend in the Niño-3.4 index (which includes the global warming trend) therefore cannot be used to argue for a trend in rainfall in Ethiopia; ENSO and global warming effects have to be investigated separately.

Marthews et al. (2015) use a large model ensemble to model the East African 2014 long rains, which was part of a joint rain-season failure in Kenya, Somalia, and southern Ethiopia. They find no evidence for anthropogenic forcing of the low rainfall, indicating that it was within the range of natural climate variability. However, a climate change signal was present in raised temperatures and increased incoming radiation. Lott et al. (2013), on the other hand, do find a climate change signal for the failure of the 2011 long rains in Kenya and Somalia. This illustrates that, even in a similar area and considering similar events, the contributing climate conditions can be very specific to an individual event, motivating a careful consideration of each new case.

There are multiple ways of defining drought, which emphasize different aspects and can lead to differences in reported conditions. IPCC (2012) outlines the common scientific definitions. Meteorological drought is a period of precipitation deficit, whereas agricultural or "soil moisture drought" concerns a deficit of soil moisture, and hydrological drought is concerned with low water availability resulting from critical streamflow, lake storage, or groundwater levels. Hydrological drought can be impacted by water abstraction and/or reservoir management (van Loon et al. 2016). Water scarcity may also sometimes be linked to socioeconomic drought, for which human activities are at least partly responsible. For agricultural or hydrological droughts, increased evapotranspiration (Teuling et al. 2013), persistence, and preconditioning are driving factors, in addition to reduced precipitation. We note that human effects such as irrigation and water extraction impede linking changes in droughts to climate change.

In this study we investigate the severity of the 2015 event mainly from the perspective of a meteorological drought. Deficit in precipitation is the main factor for droughts over Ethiopia. While anomalously high temperature can also contribute to dry surface conditions, it is not thought to be a limiting factor (T. Dinku 2016, personal communication). Precipitation anomalies and the standardized precipitation index (SPI) are standardly used as drought indices in Ethiopia. Here we choose precipitation (anomalies) as the primary variable of interest. As a secondary consideration, we also look at soil moisture anomalies to assess surface conditions representing agricultural drought.

We focus on the central–northeast region of the country, which was exceptionally dry in 2015 (Fig. 1), with the box 8°–13°N, 38°–43°E showing the spatial definition of the event to be studied. The boundaries of the box were chosen based on the homogeneity of climatological rainfall and topography. See Korecha and Sorteberg (2013) for the homogeneous rainfall zones used by the National Meteorology Agency (NMA) of Ethiopia or Diro et al. (2008) for the respective annual cycles of homogenous zones as well as maps of topography. Extending the box farther to the north or east risks introducing influences from the Red Sea; in the west topography is the natural boundary. Because of the homogeneity of precipitation in the defined box, relative anomalies are mostly similar to the absolute anomalies shown in Fig. 1. The pattern of relative anomalies is similar to the pattern of absolute anomalies, with deficits averaged over February–September up to about 50% (not shown). Fields averaged over the box will be representative of the large-scale event. We also look at the event from the local perspective, presenting results from three observational stations in the dry region.

We define the event temporally as the average precipitation of February–September 2015. This is the combination of the two rainy seasons, belg (February–May) and kiremt (June–September), which were both dry in 2015. We choose to focus our investigation on the rarity of the joint season drought, as the worst crises in food security in this region have occurred with multiple season droughts (Funk et al. 2015a), such as the back-to-back 2010 and 2011 droughts (Hillbruner and Moloney 2012). Operational Famine Early Warning Systems Network (FEWS NET) comparisons of 2015 CHIRPS data and soil moisture simulations with Ethiopian field assessments (FEWS NET 2015) indicated that many of the most severe crop and livestock losses coincided with regions experiencing water stress during both the belg and kiremt seasons.

The data and methods used are described in section 2; the observational analyses for both precipitation and soil moisture data, as well as the ENSO influence on the 2015 event, are presented in section 3; model analyses are presented in section 4; and then there follows a synthesis of the combined observational and model results (section 5) and concluding discussions (section 6).

2. Data and methods

a. Observational data

To investigate the large-scale characteristics of the drought, we use gridded observations that can be shown or averaged over the domain of interest and compared directly to model data. For the observational analysis we make use of two gridded precipitation datasets, CHIRPS (Funk et al. 2015c; data accessed online at http://climexp.knmi.nl/select.cgi?field=chirps_20_25) and Centennial Trends (CenTrends; Funk et al. 2015a; data accessed online at http://climexp.knmi.nl/select.cgi?field=CenTrendsv1).

For East Africa, CHIRPS is a state-of-the-art observational daily dataset, having been developed specifically for drought monitoring in this region (Funk et al. 2015c). It is a combination of satellite imagery with in situ station data and a high-resolution climatology, available from 1981 to the present, at a spatial resolution of 0.05° (we use the 0.25° version available online from http://climexp.knmi.nl) over the region 50°S–50°N for all longitudes. CenTrends, on the other hand, is a monthly dataset, available for 1900–2014 over the domain 15°S–18°N, 28°–54°E, and has a spatial resolution of 0.1°.

To detect trends and calculate event return periods we require a good quality and long historical dataset of monthly resolution that includes the 2015 event. Before 1960 the number of Ethiopian stations used in the CenTrends dataset is much lower (<10) compared to the number of stations after 1960 (>110), so we only use the dataset from 1960 onward.

As CenTrends and CHIRPS are based on the same underlying observational data and similar assimilation techniques we expect and verify that they are much better correlated ($r = 0.95$ for the February–September means and $r = 0.99$ for all months individually over 1981–2014 in the region of interest, with similar amplitude) in their overlap period than CHIRPS would be with other datasets [e.g., the largest correlation found for February–September means is $r = 0.90$, between CHIRPS and the GPCC version 7 (V7) monitoring product over 1981–2014 in the region of interest]. We therefore extend the CenTrends 1960–2014 series to include the study event by adding on monthly averaged CHIRPS data for 2015, and refer to the extended series as CenTrends-ext. We choose to switch from CenTrends to CHIRPS at the year 2015. This means that the trend and return period ratio will be calculated consistently from a single dataset, CenTrends, while the 2015 record value comes from CHIRPS. This same basic approach was used by FEWS NET (2015) to identify the 2015 event as "the worst drought in more than 50 years" in central and eastern Ethiopia, which expressly targeted the driest area in 2015.

In the overlap period of CenTrends and CHIRPS, 1981–2014, there is hardly a difference between the two datasets in their February–September box-averaged (see Fig. 1) precipitation time series. We therefore make no further adjustment to either dataset before their conjunction, to avoid introduction of new errors.

On a pixel by pixel basis within the box domain, the differences between the datasets at specific locations can be larger than in the box-averaged time series. When calculating maps of return periods, per pixel, the trend is again purely from CenTrends and the 2015 record from CHIRPS. In our opinion, the extended dataset is the best data currently publically available, although we note that for 2015 the density of the stations available as input for the CHIRPS dataset was quite low in Ethiopia. The box-averaged time series will be slightly superior to the field in terms of reliability, but the field is still useful for showing spatial differences.

We use station data to give insight into the drought on a local scale. Station precipitation data are obtained from both the Ethiopian NMA and the Global Historical Climatology Network (GHCN)-Monthly (GHCN-M; Peterson and Vose 1997). The latter is a worldwide collection of monthly station data (temperature, precipitation, and pressure) by NOAA/NCDC and is available on the KNMI Climate Explorer. GHCN data originate from local weather services and the Global Telecommunication System (GTS), the system used to exchange data to make weather forecasts.

Data from three local stations (Fig. 1) within the study box are analyzed—Addis Ababa (9.03°N, 38.75°E; 1898–2016), Alem Ketema (10.03°N, 39.03°E; 1974–2016), and Combolcha (11.08°N, 39.72°E; 1910–2016). Of the stations available, these three are selected for having a good combination of a relatively long time series and the fewest missing data. Data for Addis Ababa are taken from GHCN; data for Alem Ketema are from the NMA; data for Combolcha are based on NMA records but missing values are substituted from GHCN records (with no adjustment) when possible. No station has complete monthly data for 2015 and many stations miss several months in the February–September 2015 season, with the consequence that these cannot be used for return period calculations. The station at Addis Ababa, however, has just one month missing in the February–September 2015 season. We use data from this station to obtain a return period for the local event, and all three stations to make an assessment on local trends in precipitation. We replace the missing month of March in the Addis Ababa series with an estimate obtained from CHIRPS. The estimate is the CHIRPS value interpolated at the location of Addis Ababa and corrected using the linear regression of CenTrends on the Addis Ababa station series, for the month of March for years 1960–2014 (correlation coefficient $r = 0.87$).

For estimates of the temporal evolution of global mean surface temperature (GMST), which we use as a covariate in our return period analysis, we use the National Aeronautics and Space Administration (NASA) Goddard Institute for Space Studies (GISS) Surface Temperature Analysis (GISTEMP; Hansen et al. 2010). This gridded dataset is based on the GHCN version 3 (v3) point station data over land, NOAA Extended Reconstructed Sea Surface Temperature (ERSST; Huang et al. 2015) version 4 data over oceans, and Scientific Committee on Antarctic Research (SCAR) point station data for Antarctica. This method using GMST as a covariate in return period analysis has been used before in several studies (e.g., van Oldenborgh et al. 2015; Schaller et al. 2014; van der Wiel et al. 2017).

b. Soil moisture data

To analyze soil moisture conditions, we use Noah (version 3.3; Ek et al. 2003; Barlage et al. 2010), which is a water and energy balance land surface model with four soil layers, the same model that features in the FEWS NET Land Data Assimilation System (FLDAS; McNally et al. 2017). Noah has been used in several studies over East Africa (Anderson et al. 2012; Yilmaz et al. 2014), as well as other African domains (e.g., Bagayoko et al. 2006; Boone et al. 2009; McNally et al. 2015; Schüttemeyer et al. 2008), and is also used operationally in the weather, climate, and data assimilation systems at NOAA's National Centers for Environmental Prediction (NCEP). Noah is driven by the daily CHIRPS precipitation product, which has been disaggregated to a subdaily resolution as an input for the water-energy balance. This implies that the soil moisture analysis is not independent of the analysis with precipitation data. However, because soil moisture is more important for the impact of the drought than precipitation, we additionally include the Noah dataset in our analyses. This is the best we have, as the purely observational datasets we are aware of are not long enough and/or are likely not consistent enough over the data period. Here we use soil moisture from the top 10 cm of soil, as the dryness of this top layer is reported to correspond well with 2015 impacts in the field (FEWS NET 2015). We use monthly data with a spatial resolution of $0.1° \times 0.1°$, which are available for the years from 1982 to the present (McNally et al. 2016).

c. Model descriptions

Analyzing observations allows us to detect possible trends. To investigate the physical origins of a detected trend and make a statement about attribution of possible changes we need to compare data from climate model controlled simulations (e.g., simulations run with and without modeled anthropogenic emissions or forced versus not forced by observed sea surface temperatures). Climate models allow us to analyze much larger samples to reduce uncertainties and provide complete

series with no missing data. We use a set of different climate models, all of which have their specific advantages and disadvantages. In this study we investigate four different model setups, including a coupled model, an atmosphere-only model, a very large ensemble of an SST forced model, and a set of coupled global climate models. The models are described in more detail in section 4.

d. Statistical methods

The first step in the analysis is trend detection: fitting the quantity of interest to a statistical model to look for a trend outside the range of deviations expected by natural variability. In this case we study the trends of extreme droughts. In extreme value analysis, the generalized Pareto distribution (GPD) is often used to fit and model the tail of the empirical distribution for this type of event. In this region of study, however, the observational data are limited, often characterized by short records with many missing data, and we deliberately shorten the gridded data series because of probable low data quality in the beginning of the record. The resulting distributions have poorly populated tails, and consequently uncertain GPD fits. Here we choose to use a Gaussian distribution rather than a GPD, as a Gaussian uses all data rather than the sparsely populated tail and requires only two fit parameters (plus one for the trend). Using bootstrapped goodness-of-fit tests, we find that the Gaussian model fits the data sufficiently well. Factors that contribute to this are spatial averaging and limited variability compared to the mean: even the driest years are still very far from completely dry. To analyze the return periods of the observed event, we thus fit the time series of averaged February–September values (precipitation and soil moisture) to a Gaussian distribution.

The second step in an attribution analysis is the attribution of the detected trend to global warming, natural variability, or other factors, such as changes in aerosol concentration or ENSO, and requires comparing model simulations with and without anthropogenic forcing (see sections 2c and 4). Here we also take a statistical approach. In this study we investigate how the probability of occurrence of an event like the 2015 drought is independently modified by both global warming and ENSO.

In the statistical approach, global warming is factored in by allowing the Gaussian fit to be a function of the (low-pass filtered) global mean surface temperature. In the case of precipitation and soil moisture extremes, it is assumed that the scale parameter σ (the standard deviation) scales with the position parameter μ (the mean) of the Gaussian fit, and the PDF is scaled up or down with the GMST using an exponential dependency similar to Clausius–Clapeyron scaling: $\mu = \mu_0 \exp(\alpha T/\mu_0)$ and $\sigma = \sigma_0 \exp(\alpha T/\mu_0)$, where T is the smoothed global mean temperature and α is the trend fitted together with μ_0 and σ_0. A similar method has been used before for studies of extreme precipitation (e.g., Schaller et al. 2014; van der Wiel et al. 2017).

For temperature extremes, a reasonable first-order assumption is to keep the scale parameter σ fixed and then shift the whole distribution by linearly varying the position parameter μ with low-pass-filtered GMST. This results in a distribution that varies continually with GMST. This distribution can be evaluated for a GMST in the past (e.g., 1960 or 1900) and for the current GMST. A 1000-member nonparametric bootstrap procedure is used to estimate confidence intervals on the fit. This method applies to observational data and model runs with transient forcing (here EC-EARTH and HadGEM3-A), whereas return periods and risk ratios can be estimated directly between the two different climate ensembles (all forcings and natural) of the models weather@home and CMIP5.

The results from the observations and models are a set of estimates of the return period and the risk ratio (change in probability). To compare these we first have to bring them to a common time interval. We do this by assuming that the climate change from 1880 to the present corresponds to the difference between the counterfactual climate without anthropogenic emissions and the current one. This implies that we neglect the changes in natural forcings over this period, which were shown to be small in the global mean temperature (Bindoff et al. 2013). We have no reason to suspect they play a large role in droughts in Ethiopia. Second, some risk ratios are relative to 1960 instead of 1880. We transform these by assuming that the logarithm of the risk ratio depends linearly on the global mean temperature, just like for the probabilities themselves.

This gives a set of best values and uncertainty estimates of return periods and risk ratios that can be compared directly. The uncertainties in the individual estimates only include the uncertainty due to natural variability. However, the spread between the estimates also includes the model uncertainty (i.e., how well the model represents reality). A comparison between these two is made by computing the χ^2 statistic: the sum of the number of standard deviations squared that the weighted mean is away from the various estimates. We do this after taking the logarithm of the return periods and risk ratios. The fact that the uncertainty ranges of the return periods and risk ratios can be asymmetric is crudely taken into account by considering the standard deviation as half the range from the best fit to the

relevant (upper or lower) side of the 95% confidence interval. This should be compared to the number of degrees of freedom (dof) of the fit, in this case $N - 1$.

If χ^2/dof is approximately one, natural variability dominates and the weighted average is a good summary estimate of all fits. However, if it is much larger than one the spread between the values is larger than expected due to their internal uncertainty estimates and other sources of uncertainty play a role. In the case of return periods, this implies that it depends on the locations for station data, or the quality of the observations or analysis. In the case of risk ratios, it implies that the model uncertainty, the deviation between the model and reality, plays a role. The model spread and the difference between the modeled values and the observed values give an estimate of this model uncertainty. We take it into account to first order by inflating the uncertainty on the weighted average by $\sqrt{\chi^2/\text{dof}}$.

We use the same statistical procedure (Gaussian fit) to investigate the effect of ENSO on extreme precipitation in central–northeast Ethiopia. In this analysis ENSO is represented by the relative Niño-3.4 index, defined as SST in the Niño-3.4 region (5°S–5°N, 120°–170°W) minus SST averaged over 20°S–20°N to remove, to first order, the effects of global warming. The anomalies in the relative time series compare well to, for instance, the anomalies in the SOI: neither shows a trend. First we want to find out how much variance in the precipitation series is explained by ENSO in the region of study. We subtract the influence of ENSO (given by the regression slope of Niño-3.4 index on the logarithmic precipitation series) from the logarithmic CenTrends-ext precipitation series for every month in the time series and transform back into a precipitation series. Note that taking the logarithm of the precipitation series corresponds to scaling the distribution, and ensures the transformed series contains no negative values. The relative change in variance between the "before" and "after" precipitation time series gives the fraction of variance explained by ENSO. Squared correlations between logarithmic monthly precipitation and the relative Niño-3.4 index of the same month(s) can also be used to determine the explained variance over monthly time scales, but fluctuations averaged over a longer time period will lead to a reduced variance. Second, we consider the contribution of El Niño specifically in the year of interest, that is, how the event would have changed if 2015 had been an ENSO-neutral year rather than a strong El Niño year. We do this by subtracting the determined influence of ENSO from 2015 only and investigating changes to the event's magnitude and return period under ENSO-neutral conditions, with the rest of the time series unchanged.

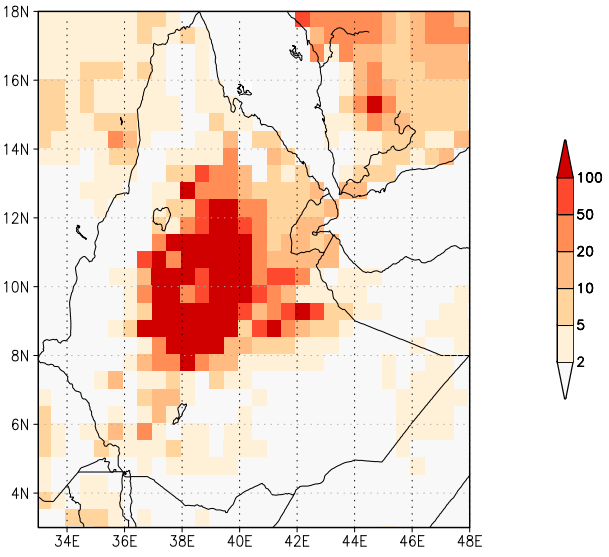

FIG. 3. Map of return period (yr) of the 2015 drought event in CenTrends-ext data.

3. Observational and soil moisture analyses: Return period and trend

a. *Analysis of gridded data*

First we apply the fit with a Gaussian distribution that scales with the smoothed global mean temperature to each grid box of the CenTrends dataset (1960–2014) and compute the return period of the 2015 CHIRPS analysis using the inverse distribution. The return periods corresponding to the anomalies of Fig. 1 are shown in Fig. 3. Note that with a series of 65 yr we cannot determine return periods of more than one century with much accuracy. The map shows that the drought was severe in about one-tenth of the country.

The longest return periods are found in the southwestern part of the defined box. Note that our box definition was not based on the event or the return period. Maps of both the trend parameter and the ratio in the box do not show any remarkable inhomogeneities (not shown).

b. *Analysis of box-averaged data*

Next we analyze the CenTrends-ext box-averaged time series. This is shown in Fig. 4 compared with the seasonal cycle for 2011–15. Figure 5 shows this time series averaged over February–September for each year, starting in 1900. Note that the analyses only use data from 1960 onward. A fit to a Gaussian distribution is shown in Fig. 6. A drought event like the 2015 drought is outside the distribution, an extrapolation gives that it is expected to happen every few hundred years [lowest estimate of 60 yr, according to the 95% confidence interval (CI)] in the current climate. The best estimate is 260 yr, but we cannot rely on this level of precision for a return period much

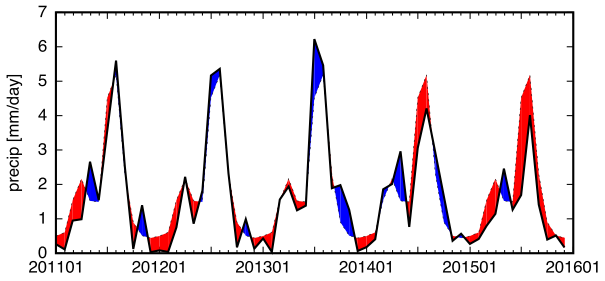

FIG. 4. CenTrends-ext time series for 2011–15 of precipitation averaged over the box shown in Fig. 1. The thick black line represents the actual precipitation time series, and the thin dashed line represents the seasonal cycle. Anomalies are taken with respect to 1981–2010. Red (blue) shading shows that it is drier (wetter) than normal.

longer than the length of the time series. In 1960 the return period of these anomalies would have been slightly longer (lowest estimate of 100 yr, according to the 95% CI, best estimate of 400 yr). The risk ratio, the factor change in the risk between the two reference years or in the probability of a similar event occurring, is thus about 1.5 but the error margins range from 0.2 to 10, which is statistically indistinguishable from zero. We conclude that we cannot detect a trend in the observations, but a trend ranging from a factor of 5 less likely to a factor of 10 more likely is not excluded at 95% confidence.

We also considered the full time series from 1900 to 2015. In this case the ratio becomes significantly positive (5.0; 95% CI: ratio of 1.6–18), which implies a drying trend. However, this may be due to the temporal inhomogeneity in the dataset.

c. *Analysis of station data*

Data from three local stations located within the study box (Fig. 1) are analyzed in the same way (Fig. 7): Addis Ababa, Alem Ketema, and Combolcha. Figure 5 shows the time series averaged over February–September for each year, showing all available data.

We could only estimate the return period for Addis Ababa, as the other series do not have enough data for 2015. The return period of an event of similar magnitude as the observed one at Addis Ababa is 3 yr (95% CI: 2–5 yr). The Gaussian fit to the data is not ideal on very small or very large time scales; however, the fit is reasonable at the intermediate time scales relevant for the 2015 event. This result deviates quite strongly from the area-averaged one. This is discussed in section 6.

As for the gridded data, we report on the trend between 1960 and 2015. No significant trend is found for Addis Ababa (also not for the years 1900 and 2015). For Combolcha there is a positive significant trend, with similar drought events being about 2 times (95% CI: 1–7 times) as likely today as in 1960. Using only data from 1953 to the present, which excludes most missing data years, gives similar results but lowers the significance. Data from Alem Ketema indicate a significant trend with a positive risk ratio of around 40 (95% CI: at least 3). Differences between these results are discussed in more detail in section 6.

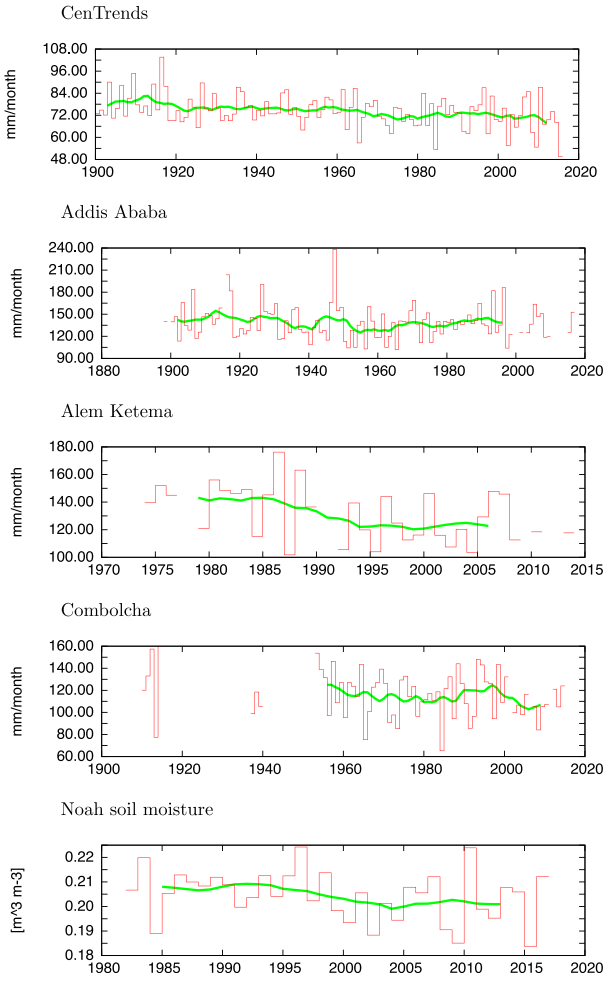

FIG. 5. Time series used in this study, averaged over February–September for all available years. (top)–(bottom) CenTrends-ext time series of precipitation averaged over the box shown in Fig. 1 and time series of precipitation for the stations Addis Ababa, Alem Ketema, and Combolcha; and Noah soil moisture averaged over the box shown in Fig. 1. The thick green lines represent the 10-yr running averages. Note that the lengths of the time series and the time axes differ.

d. *Influence of modes of natural variability*

It is well known that ENSO has a major influence on the precipitation variability in Ethiopia. Here we look at the link between the magnitude of ENSO, expressed as the monthly relative Niño-3.4 index, and the monthly CenTrends-ext precipitation in the study area. Over

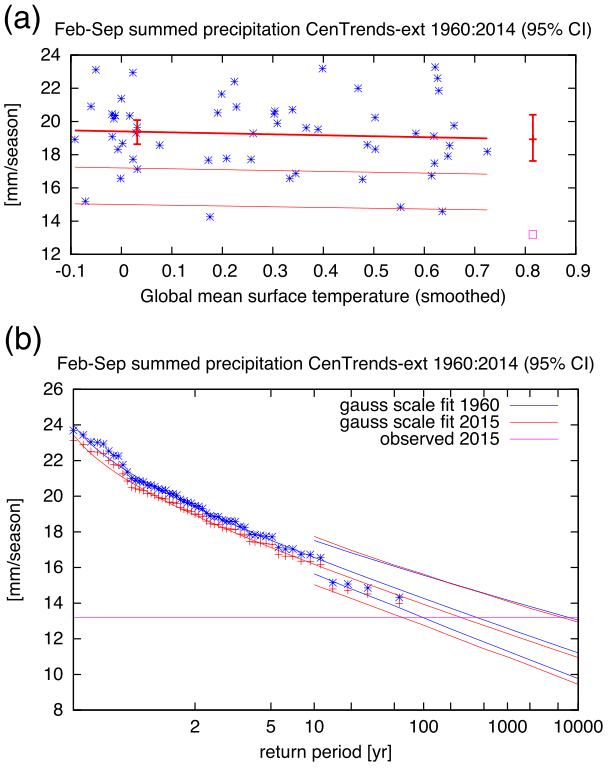

FIG. 6. Data fits and return periods of mean February–September precipitation averaged over the 8°–13°N, 38°–43°E box (Fig. 1). (a) February–September mean precipitation anomalies against the change in global mean temperature. The thick red line denotes the time-varying mean μ and the thin lines are 1σ and 2σ above, respectively. The magenta square shows the 2015 value, which was not used in the fit, and the two vertical red lines show the 95% CI of μ for the climates of 1960 and 2015. (b) Return periods for the 2015 climate (red lines) and the 1960 climate (blue lines with 95% CI). Observations are fitted to a Gaussian distribution that scales with the global mean surface temperature. The observed value in 2015 is shown by a magenta line, not used in the fit. The observations are shown twice, once shifted up to the climate of 2015 with the fitted trend (red plus signs) and once shifted down to 1960 (blue asterisks).

1960–2014, the correlation with Niño-3.4 is the largest in the months July–September, with about 36% of the variance in these months that can be explained by ENSO. As expected, the variance explained by ENSO is lower for the whole February–September season, at about 8%.

The 2015/16 event was a strong El Niño year; in the boreal summer months the relative Niño-3.4 index reached 1 K, making it about a once in 20 yr event. El Niño is therefore expected to have contributed to the drought conditions over the season February–September 2015. But what if there had been no El Niño in 2015? To investigate the influence of El Niño, we compare the severity of the observed 2015 event to that of how it might have been under ENSO-neutral conditions, leaving the rest of the time series unchanged.

Under the assumption of a linear dependence, it is shown that El Niño has a marked influence on the 2015 drought; under ENSO-neutral conditions, the total amount of precipitation is estimated to have been higher ($1.77\,\mathrm{mm\,day^{-1}}$ instead compared to $1.65\,\mathrm{mm\,day^{-1}}$ over the 8-month period). The 2015 drought would therefore likely have been less severe but still rare, with a return period of 80 yr (lowest estimate of 20 yr, according to the 95% CI), whereas with the strong El Niño of 2015 the return period is once every few hundred years (lowest estimate of 60 yr, according to the 95% CI). Choosing another Niño index does not change the result significantly.

This means that, especially in the months July–September, the February–September drought would have been less severe but still exceptional without the influence of El Niño. So El Niño enhanced the already exceptionally dry conditions in 2015. Beyond El Niño, we find no further role for decadal variability in this dataset: After subtraction of the influence of El Niño the time series is not autocorrelated anymore.

e. *Soil moisture*

We look into the severity of the drought also in terms of the soil moisture estimates. Instantaneous soil moisture reflects the balance of precipitation and evaporation over a preceding time period. Large anomalies will only be attained with persistent and anomalously dry (or wet) conditions. Linked to the integrated impact of precipitation episodes or a lack thereof, soil moisture is a measure of the longer-term water availability to crops and an indication of their condition. We still choose to analyze the 0–10-cm soil moisture (anomalies) averaged over the period February–September, as for precipitation.

The soil moisture anomalies (0–10 cm) are shown in Fig. 8. The extent of the dry anomalies is comparable to the extent of the dry precipitation anomalies shown in Fig. 1. For the analysis of the return period of the dry soil conditions we average the 0–10-cm soil moisture over the box 8°–13°N, 38°–43°E, the same as used for the precipitation analysis. The resulting time series is compared to its climatology in Fig. 9, for 2011–15, and clearly shows the impact of the failed belg and kiremt rains in creating exceptionally dry soils in 2015, with a minor recovery in May–June. The full time series averaged over February–September for each year is shown in Fig. 5.

Averaged over February–September in the defined box, the 0–10-cm soil moisture in 2015 reaches a record low for the years available (1982–present) in the dataset.

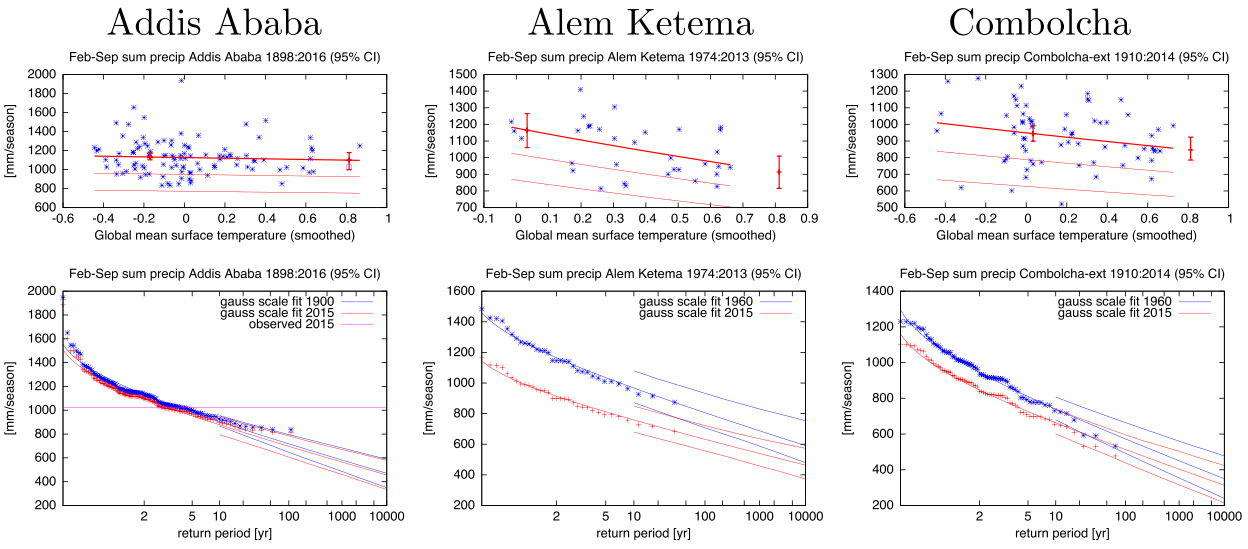

FIG. 7. As in Fig. 6, but for mean February–September precipitation for the stations (left) Addis Ababa, (center) Alem Ketema, and (right) Combolcha. Only the observed value in 2015 for Addis Ababa, not used in the fit, is shown as a magenta horizontal line.

Events like this have a return period of 25 yr (at least 5 yr with 95% CI) in the current climate (see Fig. 10 for the fit and return periods of mean February–September 0–10-cm soil moisture averaged over the defined box), and occur about 8 times (0.6–800 times with 95% CI) as frequently today than compared to the climate of 1982, which suggests a drying trend. However, the time series is relatively short and, although large, the drying trend is not quite significant. For comparison, the ratio between 2015 and 1982 calculated from the CenTrends-ext precipitation dataset when using only the years 1982–2015 is slightly above 1 and nonsignificant, with a value of 1.6 (95% CI: 0.2–33).

The drying trend is more clearly visible in the 0–10-cm soil moisture series than in the precipitation series. The soil moisture analysis thus gives (weak) evidence that a climate change signal for increased agricultural drought is present in central–northeast Ethiopia (defined box). It must be borne in mind that, because of the short soil moisture series, the signal is not very significant.

Ethiopia has warmed over the last decades, just like most of the rest of the world. Anomalously high temperatures will contribute to increased rates of evaporation and drier surface conditions, provided moisture is present for evaporation. In the introduction we stated that temperature is not thought to be a limiting factor for droughts in Ethiopia. A return period analysis of the averaged February–September temperature anomalies

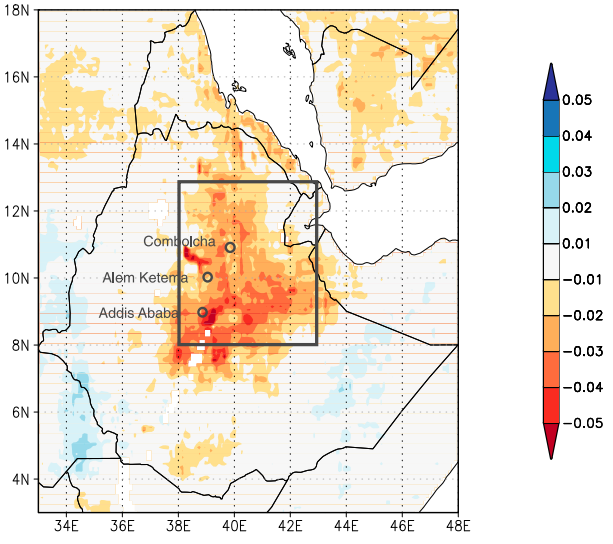

FIG. 8. Top 10-cm soil moisture content anomaly ($m^3\ m^{-3}$) w.r.t. all years, averaged over February–September 2015.

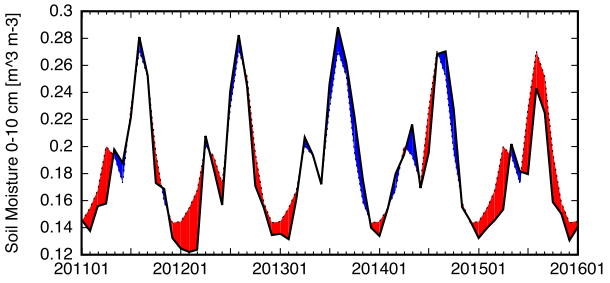

FIG. 9. Soil moisture (0–10 cm) time series for 2011–15 averaged over the box shown in Fig. 1. The thick black line represents the actual soil moisture time series, and the thin dashed line represents the seasonal cycle. Anomalies are taken with respect to 1982–2014. Red (blue) shading means that the soil is drier (wetter) than normal.

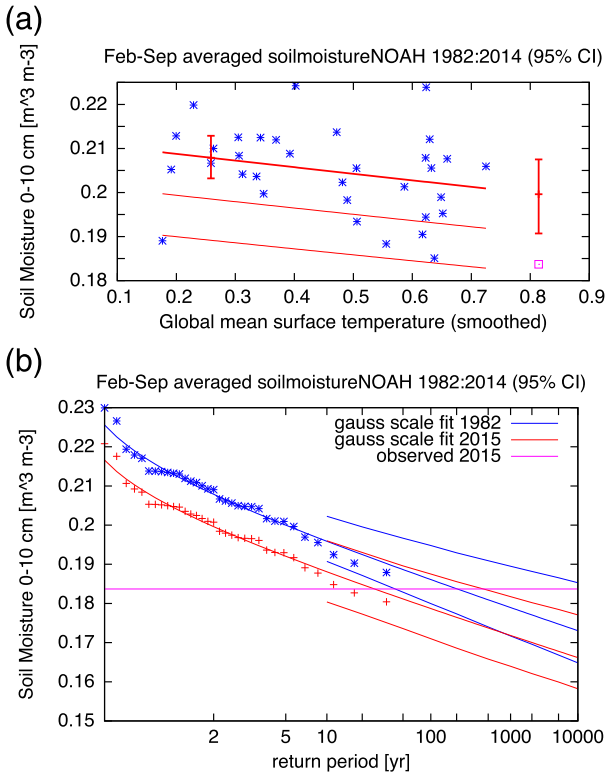

FIG. 10. As in Fig. 6, but for mean February–September 0–10-cm soil moisture averaged over the 8°–13°N, 38°–43°E box (Fig. 1) and for 2015 and 1982.

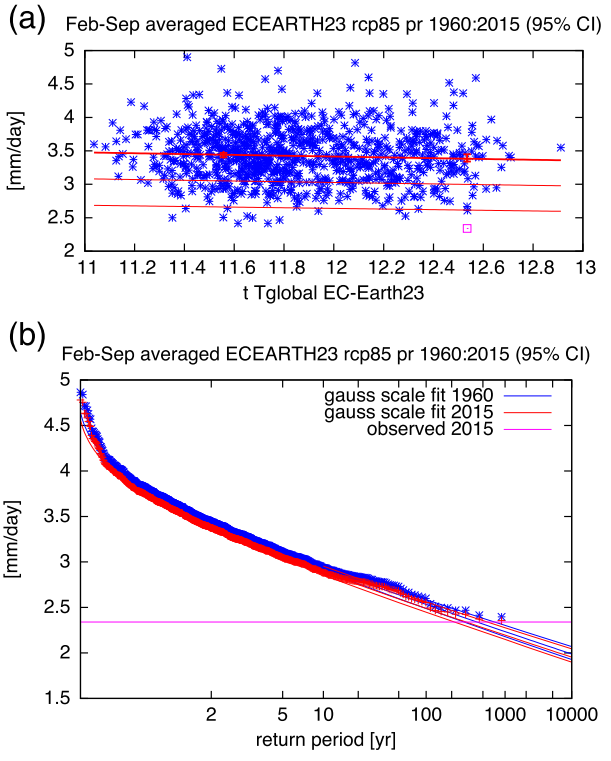

FIG. 11. As in Fig. 6, but for mean February–September precipitation in the EC-EARTH model averaged over the 8°–13°N, 38°–43°E box (Fig. 1). The observed value in 2015 is bias corrected for the averaged EC-EARTH precipitation.

(NCDC; not shown) indicates a return period of the 2015 anomaly of around 10 yr in the current climate. Thus 2015 was unusually warm, above the warming trend, but the standardized temperature anomaly is much smaller in magnitude than those of soil moisture and precipitation and probably to some extent due to the drought. The precipitation deficit was the main factor contributing to this drought. This conclusion is supported by the hydrologic contrafactual experiments in Funk et al. (2016).

4. Model analysis

a. EC-EARTH

We performed the same analysis as in the observations with the coupled atmosphere–ocean general circulation model ensemble EC-EARTH version 2.3 (Hazeleger et al. 2010). We used all 16 ensemble members covering 1861–2100 (here we use up to 2015), which are based on the historical CMIP5 protocol until 2005 and the representative concentration pathway 8.5 (RCP8.5) scenario (Taylor et al. 2012) from 2006 onward. The horizontal resolution of the model is spectral T159 truncation, which is about 125 km in the region of our interest. This means that the box we are looking at consists of 5×5 grid cells, which is expected to be large enough to describe a drought.

The EC-EARTH runs for this region overestimate the mean precipitation, and therefore also overestimate the position parameter μ in the Gaussian fit. The scale parameter σ is also overestimated. As it is assumed that the scale parameter σ scales with the position parameter μ of the Gaussian fit and the quantity σ/μ in this model is similar to σ/μ calculated from observations, the distribution can be scaled to compensate for this bias. For this reason we consider this model suitable for the analysis of the 2015 Ethiopian drought and use a simple scaling factor of 1.4 for the 2015 precipitation value in the model.

In the EC-EARTH model a drought like in 2015 is very extreme and would occur every 300 yr (95% CI: 200–550 yr) (see Fig. 11). While we have data available from 1860, we find that the response of precipitation to GMST is different for 1860–1960 than for 1960–2015. This means that the natural response is not similar to the response to greenhouse gases and it is not appropriate to use the combined period for a linear trend analysis. As we can only compare 1960–2015 with observations, we use only these years for the analysis of the trend. The

return period of a drought like in 2015 would have been 400 yr (95% CI: 300–700 yr) in 1960. This gives a ratio of 1.4 (95% CI: ratio of 0.9–1.8) between 2015 and 1960. This is consistent with the results found in the observational analysis: a nearly significant trend toward less precipitation. The correlation with El Niño in the months July–September is only −0.19 and therefore is not studied further.

b. HadGEM3-A

In the European Climate and Weather Events: Interpretation and Attribution (EUCLEIA) project, the Met Office model HadGEM3-A (A. Ciavarella 2017, unpublished manuscript) was run in atmosphere-only mode at high resolution (N216, about 60 km). This was done with observed forcings and sea surface temperatures (SSTs) ("historical") and with preindustrial forcings and SSTs from which the effects of climate change have been subtracted ("historicalNat"). The latter change has been estimated from the ensemble of coupled climate simulations from phase 5 of the Coupled Model Intercomparison Project (CMIP5) [for details, see Stone and Pall (2016, manuscript submitted to *J. Adv. Model. Earth Syst.*)]. The simulations were made as an ensemble of 15 realizations for the period 1960–2015 and as an ensemble of 105 realizations for the period 2014–15 for the same forcings. The data are freely available for noncommercial use.

The HadGEM3-A runs for this region overestimate the mean precipitation only slightly, and therefore also only slightly overestimate the position parameter μ in the Gaussian fit. The scale parameter σ is, however, overestimated strongly. The variance in this model in this region is too high compared to the model mean and the quantity σ/μ is not within the 95% CI of the quantity estimated from observations. For this reason we do not consider this model suitable for this analysis and do not use it for calculations on return periods.

Considering the trend in the model, the historical runs show a negative trend. However, the historicalNat runs show an even stronger negative trend. This means that the influence of natural forcings and model drift are responsible for the trend in precipitation in this region, and not climate change. The difference in trend between the historical and historicalNat runs is even slightly positive, which points to more precipitation today than there was in the past. However, we do not know the reason for the large trends in both ensembles, lessening our confidence in the results.

c. weather@home

Using the distributed computing framework "climate*prediction*.net" atmosphere-only general circulation modeling weather@home (Massey et al. 2015), very large ensembles of regional climate model simulations at 50-km resolution over a large African region are available from 1986 to the present. Driven by observed SSTs and sea ice conditions from Operational Sea Surface Temperature and Sea Ice Analysis (OSTIA; Stark et al. 2007), possible weather under observed climate conditions is simulated. Corresponding to these simulations of possible weather in East Africa under current climate conditions ("all forcings"), ensembles of counterfactual simulations of possible weather in a world as it might have been without anthropogenic climate drivers ("natural") are simulated for 2015. To remove the anthropogenic signal from the counterfactual simulations the atmospheric composition is held at preindustrial levels of greenhouse gases and aerosols and the estimated pattern of warming from the observed SSTs is removed. Patterns of warming in the SSTs are obtained by subtracting various estimates of the difference between preindustrial and present-day conditions from the ensemble of opportunity CMIP5 (Taylor et al. 2012). [See Schaller et al. (2014) for details.]

Evaluating the performance of the model to estimate droughts in the Greater Horn of Africa, Marthews et al. (2015) found a dry bias in the drought region of the 2014 drought. In contrast, the more northerly region affected by drought in 2015 shows a wet bias. While the mean of the simulations is too high, the distribution of extremes is comparable to observations (although this depends on which observational dataset is used), in particular in the belg season. Given that we only compare the relative results of the all forcings ensemble and the natural ensemble we do not attempt to correct for the offset in the mean but use the uncorrected model.

The weather@home simulations provide a very different picture for the two rainy seasons. Whereas in the belg season (February–May) both distributions are identical (not shown), the kiremt season (June–September) does show an effect due to anthropogenic climate change increasing the risk of extremely dry seasons. What is a once in 100 yr event in June–August in the world we live in would have been an extremely rare event in the world that might have been with a return period of a thousand years (see Fig. 12), leading to a changing risk of a factor of 11 (95% CI: factor of 5–35).

The results of the analysis of the rainfall averaged over both seasons are qualitatively identical to those of the kiremt season but showing overall smaller signals (see Fig. 12). The increase in risk for the once in 100 yr event for both seasons is a factor of 2.3 (95% CI: factor of 1.1–5.1). A once in 100 yr event would have been a once in 230 yr event and the once in 260 yr event would have been a once in 3000 yr event, making the event 13 times (95% CI: 2–20 times) more likely under current climate conditions as observed in 2015 in the weather@home model.

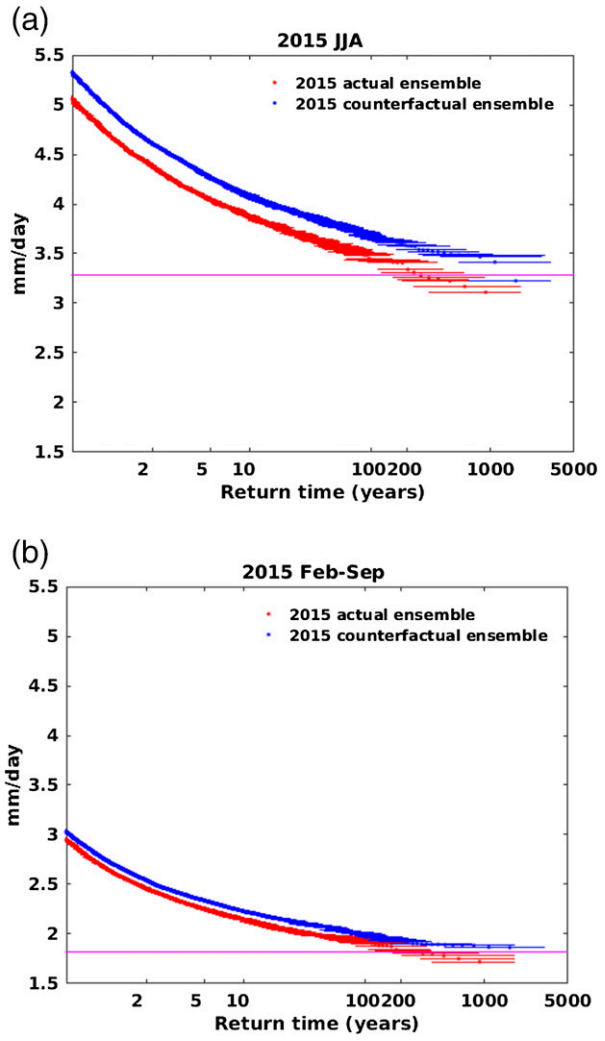

FIG. 12. Seasonal return period plot of mean precipitation (mm day^{-1}) over Ethiopia, averaged over the 8°–13°N, 38°–43°E box, for the rainfall periods (a) June–August and (b) February–September. The actual (red) and natural (blue) simulations with 3000–6000 simulations are represented with dots while the horizontal lines depict the 95% CI of the sampling uncertainty. The pink horizontal line represents the once in 260 yr event.

d. CMIP5

The models were evaluated based on their ability to capture the observed distribution of February–September precipitation anomalies. First the observational and model data were all converted into anomalies from a 1961–90 climatology (with historicalNat and RCP8.5 simulations computed as anomalies from their equivalent historical run). This comparison was made using the CenTrends dataset and the historical model simulations (for 1951–2005) with the requirement that a Kolmogorov–Smirnov test does not show significant differences ($p < 0.05$) in at least two-thirds of available historical simulations. Eleven models passed this test and were used in the attribution step (see Table 1).

The statistical distributions of February–September rainfall anomalies were compiled for the natural climate ensemble (historicalNat; 1901–2005), the current climate (RCP8.5; 2006–26), and the future climate of 2050 under continued high greenhouse gas emissions (RCP8.5; 2040–60) (see Fig. 13). The 2015 event was a very extreme event in the CenTrends-ext dataset and the return periods of this event are highly volatile and uncertain for this reason. In the CMIP5 ensemble we therefore do not look at these return periods but instead investigate changes in the return period of the historical 20% precipitation deficit. The return period for this threshold is 30 yr in the current climate (90% CI: 16–62 yr). There is almost no change when we compare this to past runs (30 yr; 90% CI: 18–68 yr) or to runs for the future in the year 2050 (30 yr; 90% CI: 16–91 yr). The risk ratio between 2015 and a natural world is between 0.42 and 1.83 (90% CI). So our analysis shows no significant change in the likelihood of precipitation deficits. Thus, using our multimodel analysis we cannot detect a clear climate change influence on the 2015 Ethiopian drought event.

5. Synthesis

In 2015, Ethiopia's central–northeast regions suffered from two consecutive poor rainy seasons: the belg rains (February–May) were declared to have failed and the kiremt rains (June–September) were late and sporadic, leading to drought conditions and failed harvests. Adopting the meteorological drought perspective, we defined the event for investigation as the February–September precipitation averaged over the area 8°–13°N, 38°–43°E. A multimethod attribution was performed, based on observational precipitation analyses (CenTrends extended with CHIRPS and station data), climate model simulations of precipitation (EC-EARTH, weather@home, CMIP5, and HadGEM3-A) to examine the rarity and changes in probability of such a joint season drought, as well as the influence of El Niño. For comparison, we repeated the analysis for February–September 0–10-cm soil moisture anomalies (Noah forced soil moisture simulations) to assess surface conditions representing agricultural drought.

An overview of the multimethod results for return periods and trends (risk ratios) is shown in Figs. 14–16. Return periods could only be obtained for the gridded observational precipitation dataset CenTrends-ext, for a single station (Addis Ababa), and for soil moisture. As

TABLE 1. Climate model simulations used in this study. Models shown in boldface passed the validation test and were used in the event attribution analysis. (Expansions of acronyms are available online at http://www.ametsoc.org/PubsAcronymList.)

Model name	Modeling experiment		
	Historical	HistoricalNat	RCP8.5
ACCESS1.3	**1, 2, 3**	**1**	**1**
BCC_CSM1.1	**1, 2, 3**	**1**	**1**
CanESM2	**1, 2, 3, 4, 5**	**1, 2, 3, 4, 5**	**1, 2, 3, 4, 5**
CCSM4	**1, 2, 3, 4, 5, 6**	**1, 2, 4, 6**	**1, 2, 4, 6**
CESM1(CAM5)	**1, 2, 3**	**1, 2, 3**	**1, 2, 3**
CNRM-CM5	**1, 2, 3, 4, 5, 6, 7, 8, 9, 10**	**1, 2, 4**	**1, 2, 4**
CSIRO Mk3.6.0	1, 2, 3, 4, 5, 6, 7, 8, 9, 10	1, 2, 3, 4, 5	1, 2, 3, 4, 5
GFDL CM3	1, 2, 3, 4, 5	1	1
GISS-E2-H	1, 2, 3, 4, 5	1	1
GISS-E2-R	**1, 2, 3**	**1**	**1**
HadGEM2-ES	**1, 2, 3, 4, 5**	**1, 2, 3, 4**	**1, 2, 3, 4**
IPSL-CM5A-LR	1, 2, 3, 4, 5, 6	1, 2, 3	1, 2, 3
IPSL-CM5A-MR	1, 2, 3	1	1
MIROC-ESM	**1, 2, 3**	**1**	**1**
MRI-CGCM3	**1, 2, 3**	**1**	**1**
NorESM1-M	**1, 2, 3**	**1**	**1**

the model return periods depend on the calibration to the CenTrends data they do not add independent information and are not shown.

For the CenTrends-ext dataset we found a return period over the study domain 8°–13°N, 38°–43°E of a few hundred years, with a lowest estimate of 60 yr (according to the 95% CI). The return period at the station Addis Ababa was found to be only 3 yr (95% CI: 2–5 yr). The difference is visualized in Fig. 14. This difference is due to a few reasons, including scarcity of the data, point station data versus gridded data, and differences over the area over which we averaged. We discuss this in more detail in section 6.

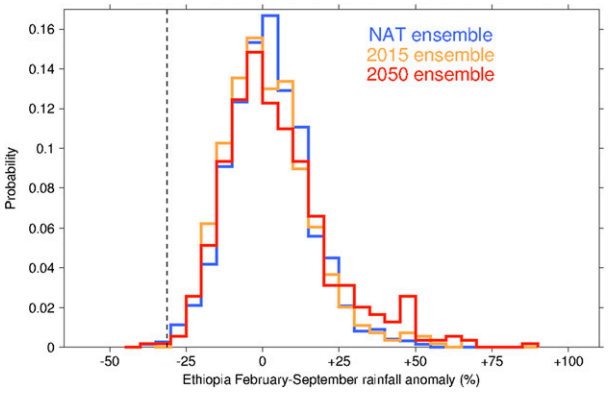

FIG. 13. PDFs of Ethiopian February–September rainfall anomalies in the all-forcings ensemble, representing the world during 2006–26 (orange) and the historicalNat-forcings (NAT) ensemble (blue). Also shown is the ensemble of 2040–60 (red) assuming continued high greenhouse gas emissions under the RCP8.5 scenario. The 2015 rainfall anomaly is shown (dashed line).

For soil moisture data the return period is about 25 yr (95% CI: 5–440 yr).

The trend between 1960 and 2015 was estimated in additional datasets, including two extra station datasets and three different model settings. In the CenTrends-ext dataset from 1960–2015 we find a nonsignificant trend with a risk ratio (ratio of the probability today and the probability in the climate of 1960) of 1.5 between 2015 and 1960, with error margins ranging from 0.2 to 10 (see Fig. 15). The Addis Ababa station (1898–2016) also shows no significant trend (also not over the common period 1960–2015), but the Combolcha station (1910–2014) shows an increasing risk of dry extremes with a risk ratio between 2015 and 1960 of 2 (95% CI: ratio of 1–7). At the station Alem Ketema (1974–2013) the trend is even stronger: an event like the drought in 2015 is found to happen at least 3 times more often today than it was around 1960. In spite of the large uncertainties, these different trend estimates are statistically not

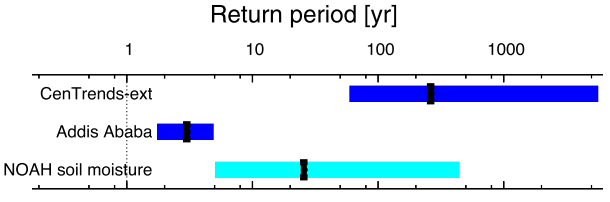

FIG. 14. Return period of the 2015 drought in the area-averaged analysis of CenTrends extended with CHIRPS (see text for details), at the station of Addis Ababa, and in the 0–10-cm soil moisture dataset generated with the Noah land surface model. Note that the measures do not estimate the same quantity as they include area-averaged precipitation, station precipitation, and area-averaged soil moisture data.

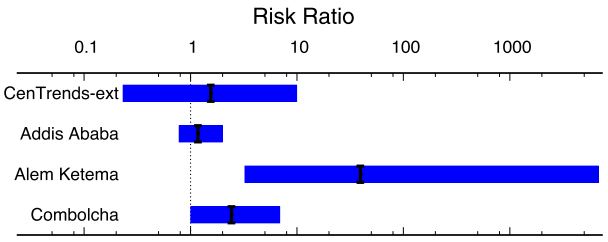

FIG. 15. Risk ratios (change in probability between 2015 and 1960) in observational estimates. The spread between the stations and the area-averaged estimate is so large that it is very unlikely they are estimates of the same underlying quantity: the trend in drought was different at the different locations (or the station series are not homogeneous). Note that the measures do not estimate the same quantity as they include area-averaged precipitation and station precipitation data.

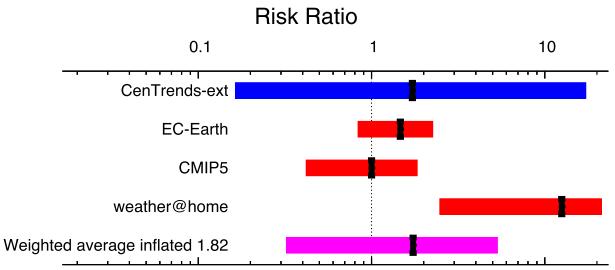

FIG. 16. Synthesis of the area-averaged risk ratio (change in probability between 2015 and 1880) results for observed precipitation (dark blue) and climate model ensembles (red). The ranges are not compatible with each other, pointing to model uncertainty playing a role over the natural variability. The weighted average (magenta) has been inflated by a factor of 1.82 to account for the model spread. Note that both the scale of this figure and the base for the risk ratio differ from that in Fig. 15.

compatible (χ^2/dof = 3.0, assuming lognormal distributions and treating the lower and upper bounds as different; see section 4d). This means that they are not estimates of the same underlying quantity, but the trend in drought was very different in the different locations of the stations. The relatively short time series of Alem Ketema could also be influenced more by decadal variability, which is not considered in the estimation of the uncertainties. Finally, the observations could contain inhomogeneities. For further analysis we only consider the area-averaged CenTrends value, as this corresponds to the area impacts and to the model output.

The EC-EARTH model shows a nonsignificant drying trend with a ratio between 2015 and 1960 of 1.4 (95% CI: ratio of 0.9–1.9). In the weather@home ensemble, both the joint season and the belg and kiremt seasons are discussed separately. We find no significant trend in the belg season but a drying trend in the kiremt season. The ratio between 2015 and preindustrial for the joint season is also significant, with a value of 2.3 (95% CI: 1.1–5.1). The CMIP5 ensemble shows no significant trend, either in the present or in the future climate runs. Finally, the HadGEM3-A was not realistic enough in this region to be used in this analysis. As can also be seen by eye from Fig. 16, these model results are statistically not compatible with each other (χ^2/dof = 3.3), which implies that the differences are due to not only natural variability but also model spread.

The fact that observations show a ratio between 2015 and 1960 ranging from a factor of 5 less likely to a factor of 10 more likely is not inconsistent with the model results. For the CMIP5 ensemble and the weather@home ensemble, the risk ratio is defined as the change in probability between 2015 and preindustrial conditions. To synthesize all results using comparable base periods, we transform all risk ratios to be relative to 1880. Although there are differences in precipitation trends between the models, the confidence interval obtained from CenTrends-ext virtually encompasses the confidence intervals of all model results. The trends in droughts in the models between the current climate and preindustrial range from a factor of 2 less likely (CMIP5) to a drying trend of 20 times more likely (weather@home). A weighted average of the CenTrends observational estimate and the three models gives a risk ratio of 1.8 (risk ratio here is defined as the change in probability between 2015 and 1880), but inflating the uncertainty range to make χ^2/dof one to account for the model spread we obtain an uncertainty range of 0.3–5 that easily encompasses no change (the risk ratio being defined as the change in probability between 2015 and 1880). This implies that although the observations and models tend to a somewhat increased probability of drought, we cannot attribute the observed drought to climate change as a trend toward less drought is also compatible with the observations and model results.

In addition to a trend analysis on precipitation, we did an analysis of the trend in 0–10-cm soil moisture. Results indicate a drying trend with a risk ratio of 8 between 2015 and 1982, although the trend is not significantly different from zero (risk ratio not significantly different from one) because of the short time series. This means we cannot attribute the agricultural drought to a trend either.

Finally the influence of ENSO was studied in the observational dataset CenTrends-ext. In this dataset the relative Niño-3.4 index explains about 36% of the variance in July–September (8% over February–September). The precipitation would have been higher if 2015 had been an ENSO-neutral year: 1.77 instead of 1.65 mm day^{-1}. The return period of such an event would have been about 3 times lower in an ENSO-neutral year, with a best estimate of 80 yr (>20 yr). This means that El Niño has enhanced

the drought, but even without El Niño the drought would still have been extreme. The influence of ENSO could not be studied in the models, as EC-EARTH did not have the correct teleconnection and weather@home was only run for 2015. The CMIP5 models each have different teleconnections and we have not attempted to analyze these.

6. Discussion and conclusions

We estimated the return period of the 2015 drought from station data and a comprehensive gridded analysis, CenTrends and CHIRPS, and trends in the probability of a drought like the one of 2015 or worse from these observations and various large ensembles of climate models. This immediately brings up the first problem we encountered: the poor availability of meteorological observations in Ethiopia hinders the effort to analyze droughts in Ethiopia, both by international and Ethiopian scientists. A collaborative effort combining knowledge from the local and global communities gives the best results, but is still hampered by the lack of data from ground observations.

As mentioned by Singh et al. (2016), we iterate that results on the return periods in particular can be sensitive to choices made for the selected approach, such as the spatial and temporal event definition and the dataset(s) used for analysis. However, as data are sparse in Ethiopia, we use the datasets that are available, even with their limitations. The limitations and implications for the results are discussed below.

In this study we chose to use CenTrends-ext as our primary observational dataset, to which we compare all other observational and model data results. It covers the entire region of interest and, as a gridded dataset, it also facilitates comparisons with model fields. It uses satellite data to fill in the recent lack of station data.

We experimented with two small changes to the event definition. In the first one we extended the box farther north, to 14°N. In the second test we used 7 months instead of 8, examining February–August and March–September. The spatial test showed no difference in risk ratio and only a small decrease of the lower bound of the return period. The temporal test indicated that excluding February indicates a slightly lower nonsignificant risk ratio, with CI between 0.1 and 6 instead of between 0.2 and 10. Excluding September resulted in a decrease in the lower bound of the return period to 30 yr instead of 60 yr. These small differences with the original results are to be expected when choosing a different event definition. Overall the results are not very sensitive to the spatial and temporal definition.

The large difference in the estimated return period between CenTrends-ext (a few hundred years) and the station Addis Ababa (about 3 yr) merits discussion. First, data are very scarce in Ethiopia, especially in 2015. The density of stations in the CHIRPS dataset in 2015 was very low. For instance, for the months February–May, at the time the CHIRPS dataset was made, the Addis Ababa station data were not yet available, so no station data were assimilated in CHIRPS for the station Addis Ababa and it relied wholly on satellite data, which could make the CHIRPS value substantially lower than the station value and lead to an erroneously large CenTrends-ext return period. However, it is worth noting that satellite-only version of the CHIRPS dataset (named CHIRP) has been shown to correspond closely with Ethiopian gauge-based estimates (Dinku et al. 2017, manuscript submitted to *Quart J. Roy. Meteor. Soc.*). In addition, it should be noted that subsequent analyses carried out by FEWS NET, in collaboration with the Ethiopian National Meteorology Agency, with a robust set of gauge observations have identified a large negative deficit, similar in value to that identified by CHIRPS data. Note also that the station data are not without problems; all station data we have access to are missing at least one monthly value in February–September 2015. In the Addis Ababa series, we replaced the missing month of March with an estimate obtained from CHIRPS. If the replacement value was too large, it would lead to a drought of lower severity and erroneously reduce the return period. However, compared to the series obtained by replacing the March value with the lowest possible value, zero, the return period is only decreased by about 1 yr. Our handling of missing data therefore cannot explain the hundredfold difference in return periods between CenTrends-ext and the station Addis Ababa. It is also possible that the daily precipitation series used to create the GHCN-M dataset by NOAA/NCDC suffers from incomplete records and we do not know how the handling of missing daily data values (if present) would affect confidence on the monthly values.

Second, differences will stem simply from inhomogeneity of the drought conditions in the study area or the patchy nature of this drought: there is a large difference in the magnitude of the 2015 anomaly for the region as a whole ($-0.75\,\mathrm{mm\,day^{-1}}$, or standardized anomaly of $-2.73\,\mathrm{mm\,day^{-1}}$), compared to the 2015 anomaly at Addis Ababa station ($-0.37\,\mathrm{mm\,day^{-1}}$, or standardized anomaly of $-0.61\,\mathrm{mm\,day^{-1}}$). An additional confounding factor is the potential difference in variance for a rainfall point observation (a gauge at Addis Ababa) versus the variance of rainfall averaged over a large study area, such as that used in this analysis. The interannual standard deviation of our areal-averaged February–September rainfall is $0.28\,\mathrm{mm\,day^{-1}}$ on a mean of $2.7\,\mathrm{mm\,day^{-1}}$ (10%), whereas the corresponding standard deviation for Addis Ababa is larger, at

0.61 mm day^{-1} on a mean of 4.6 mm day^{-1} (13%). Higher local variances can make it difficult to detect changes in in situ gauge time series. This is a common problem when working with precipitation, as local variances at stations are almost always larger than variances of areal averages, because of spatial averaging over scales larger than the small spatial autocorrelation reducing the variability. Another important factor is the inhomogeneous nature of the drought. The correlation between February–September Addis Ababa rainfall and the areal average is only $r = 0.5$, so only one-quarter of the variance is in common. Note that the anomalies, means, and standard deviations in this paragraph are given with respect to 1960–2014.

Return periods for the 2015 meteorological drought are also reported by FEWS NET (2015), based on CenTrends (years 1960–2014) and CHIRPS (year 2015) averages for March–September, and by Singh et al. (2016), based on CHIRPS (years 1981–2015) averages for February–August. Both use a region that overlaps with the one used here, but with boundaries determined by the drought event of interest (which in general will serve to make the reoccurrence of such an event rare by construction and should therefore be combined with a spatial analysis: how often would one expect a return period like this in a wider region?). Minimum return periods are defined by the actual length of time since the recent record was last surpassed, which in both cases is limited by the length of the dataset, respectively around 50 and 30 yr. Despite the differences in the defined event area and season and method, these simple measures reported for the lower bound of the return period are of the same order of magnitude as that found here (60 yr). While our multimethod approach partially sampled method-based uncertainty and that due to natural variability, it fixed the event definition. The above comparison hints that, in this case study, our results are not especially sensitive to the choices for the spatial or temporal large-scale event definition but that the return period likely hinges more on the choice of data series used and the quality of that data.

FEWS NET (2015) also reports on joint-season (March–September) top 10-cm soil moisture conditions based on the same FLDAS model, mapping local anomalies expressed as the actual return periods within the dataset, with some wide areas in the central–northeast sector experiencing at least once in 30 yr dryness. The spatial distribution compares very well with our map of return periods of the 2015 conditions (not shown), which is to be expected as the source data and season are nearly the same, except that the driest areas within the study domain experience at least once in 60 yr dryness. This is because, unlike the method used in FEWS NET (2015), our statistical approach allows us to estimate return periods beyond the length of the almost 30-yr dataset, reliably up to around 2–3 times its length. This return period, however, depends strongly on whether we assume a stationary climate or assume the strong fitted trend. In the latter case, for our domain-averaged time series, we obtain a return period of roughly 25 yr, with a lower boundary of the 95% CI of 5 yr in the current climate. Under the assumption that the trend is in fact zero (the fit is not significantly different from zero), the return period is roughly 70 yr (lower boundary of the 95% CI of 23 yr).

We are aware of the fact that the choice of using CenTrends-ext for the calculation on the return period of the 2015 drought has a large influence on the conclusion of the extremity. However, the large CHIRPS 2015 values do corroborate local reports from the field (FEWS NET 2015). Considering the above discussion, we conclude that the return periods we have for the gridded dataset are the best estimates we have for the region of study. We recommend placing most confidence in the conservative lower bound of the 95% confidence interval (based on internal variability) of 60 yr.

It is important to realize that the statements on the severity of the 2015 drought here relate to the central–northeast region alone. Statements for the 2015 drought based on similar regions suggest that the lower limits on the return period are around 30–50 yr. Some have therefore (or for other reasons) concluded that the 2015 drought was as severe as or worse than the 1984 drought; however, the earlier drought occurred over a different and much larger area and consequently impacted more people (Singh et al. 2016). The region analyzed here is also the region with the largest impact from El Niño, which intensified the drought but did not alone cause it. Rainfall in Ethiopia is not completely forced by SSTs but also has a large unpredictable component. Correlations with global SST do not show obvious other patterns than El Niño. The correlations between the 1981–2015 July–September rainfall simulated by SST-forced GCMs from NOAA's Earth Systems Research Laboratory (https://www.esrl.noaa.gov/psd/repository/alias/facts/) and CHIRPS over Ethiopia (~0.5), which is what we expect from the correlation with Niño-3.4, although this may also be due to model deficiencies.

Furthermore we want to emphasize that the observational data for 2015, which suffers from missing station records, has no influence on the analysis of the trend, and only a small influence on the risk ratio. So although values for the return period cannot be given with high certainty, the results on the trend and risk ratio are still reliable.

We show the whole CenTrends-ext time series, starting in 1900, but we only analyze data from 1960 onward. As explained in section 3 we do not trust the data before 1960 because of a large increase in number of stations that contribute to the dataset. Using all data would result in a significant drying trend (risk ratio of 5; 95% CI: ratio of 2–18). However, we do not know whether this is a real signal or a spurious trend that stems from the change in stations used. The station Combolcha that has a comparable length shows a lot of missing data between 1910 and 1953. However, omitting the data from 1910 to 1952 only lowers the significance and does not change the risk ratio or return period themselves.

The difference in risk ratio between the two stations with a long time series Addis Ababa (no significant trend) and Combolcha (risk ratio of 2) likely stems from the difference in location. There are very local controls on rainfall in Ethiopia, and the fact that Addis Ababa was elected to be the location for a capital is probably also based on rainfall being relatively stable in Addis Ababa. In Addis Ababa the seasonal cycle shows more rain in May and June than in the same months in Combolcha. In Combolcha we find a drying trend in these relatively drier two months May and June that link the ''belg'' season with the ''kiremt'' season. We do not find such a trend in the Addis Ababa station data. This shows that the complexity of Ethiopia's topography and climate can cause relatively large local differences.

The combination of model and observations gives as best estimate that the probability of dry extremes in north-central Ethiopia has increased by a factor of between 0.3 and 5. This range encompasses one, which indicates no change, but does not exclude a small decrease in probability or a larger increase in probability, up to a factor of 5 more likely. The large uncertainties result from the short observational series (1960–2014) and the model spread as well as the large interannual variability in the region. Trend analyses featured in other studies using observational data do not bring to light significant drying in this region (Cheung et al. 2008; Williams and Funk 2011; Jury and Funk 2013; Viste et al. 2013; see introduction). The drought can also be seen in soil moisture estimates reconstructed by models nudged with meteorological analyses. However, this record is also too small to attribute this aspect of the drought to climate change: although the central value points to an increase in probability, the uncertainty range again encompasses no change.

The role of aerosols has not been quantified in this study. It is known that aerosols are a major driver of precipitation in the monsoon regions (e.g., Polson et al. 2014), which could also be the case for Ethiopia, being located on the fringe of the African monsoon region. Simple correlations of our observed precipitation series with the TOMS aerosol data (1980–2001) indicate a weak negative correlation for local and North African aerosols mainly in July–August, and a weak positive correlation for Asian aerosols in May; the recent reduction in North African aerosols may act to partly mask a stronger drying trend since the late 1980s in the February–September observed averages. This dataset is, however, too short and noisy to be relied upon. Furthermore, the relation between aerosols and precipitation is complex, involving far-field teleconnections and indirect effects. An in-depth accounting of the effect of aerosols is therefore beyond the scope of this study. It has been hypothesized by Rowell et al. (2015) that the recent increase in Asian emissions or the decline in European and North American emissions might be a driver of the East African long rains (March–May), but that ''understanding and modeling of the role of changing anthropogenic aerosol emissions is currently inconclusive'' (p. 9781).

For the Ethiopia February–September rainfall sum there is no East Africa climate paradox: the trends in observations and climate models are completely compatible within the uncertainties due to natural variability (Fig. 16). The models are not compatible among themselves within this variability, so we have to take model uncertainty into account (as in most drought analyses).

Finally we remark that a fuller coverage of the 2015 drought would also address the vulnerability that results from the hydrological drought—that is, the decrease in the availability of stored water including the effects of increased extraction—but this is beyond the scope of this article, if not virtually all current attribution studies. Ethiopia is the second most populous country in sub-Saharan Africa and its population growth rate is near 2.5%. As Ethiopia's population continues to grow, vulnerability and exposure to droughts will increase even if the evidence implies these droughts will not occur more frequently. This underscores the need for Ethiopia to prioritize adaptation to climate extremes while continuing on its rapid development path.

Acknowledgments. This study was conducted as part of the Raising Risk Awareness project and the World Weather Attribution activity coordinated by Climate Central. We thank the National Meteorology Agency of Ethiopia for supplying additional station precipitation data and acknowledge NOAA's National Centers for Environmental Information for the production of the GHCN-M dataset. For their technical expertise, we thank our colleagues at the Oxford eResearch Centre, A. Bowery, M. Rashid, S. Sparrow, and D. Wallom, and

the Met Office Hadley Centre PRECIS team for their technical and scientific support for the development and application of weather@home. This research was done as part of the Raising Risk Awareness project, a partnership between the World Weather Attribution (WWA) Initiative and the Climate and Development Knowledge Network (CDKN) and also supported in part by the EU project EUCLEIA under Grant Agreement 607085.

REFERENCES

AKLDP, 2016: El Niño in Ethiopia, 2015–2016: A real-time review of impacts and responses. USAID Agriculture Knowledge, Learning, Documentation and Policy Project 663-13-000006, 28 pp., http://www.agri-learning-ethiopia.org/wp-content/uploads/2016/06/AKLDP-El-Nino-Review-March-2016.pdf.

Anderson, W. B., B. F. Zaitchik, C. R. Hain, M. C. Anderson, M. T. Yilmaz, J. Mecikalski, and L. Schultz, 2012: Towards an integrated soil moisture drought monitor for East Africa. *Hydrol. Earth Syst. Sci.*, **16**, 2893–2913, https://doi.org/10.5194/hess-16-2893-2012.

Bagayoko, F., S. Yonkeu, and N. C. van de Giesen, 2006: Effect of seasonal dynamics of vegetation cover on land surface models: A case study of Noah LSM over a savanna farm land in eastern Burkina Faso, West Africa. *Hydrol. Earth Syst. Sci. Discuss.*, **3**, 2757–2788, https://doi.org/10.5194/hessd-3-2757-2006.

Barlage, M., and Coauthors, 2010: Noah land surface model modifications to improve snowpack prediction in the Colorado Rocky Mountains. *J. Geophys. Res.*, **115**, D22101, https://doi.org/10.1029/2009JD013470.

Bindoff, N. L., and Coauthors, 2013: Detection and attribution of climate change: From global to regional. *Climate Change 2013: The Physical Science Basis*, T. F. Stocker et al., Eds., Cambridge University Press, 867–952.

Boone, A., and Coauthors, 2009: The AMMA Land Surface Model Intercomparison Project (ALMIP). *Bull. Amer. Meteor. Soc.*, **90**, 1865–1880, https://doi.org/10.1175/2009BAMS2786.1.

Camberlin, P., 1997: Rainfall anomalies in the source region of the Nile and their connection with the Indian summer monsoon. *J. Climate*, **10**, 1380–1392, https://doi.org/10.1175/1520-0442(1997)010<1380:RAITSR>2.0.CO;2.

Cheung, W. H., G. B. Senay, and A. Singh, 2008: Trends and spatial distribution of annual and seasonal rainfall in Ethiopia. *Int. J. Climatol.*, **28**, 1723–1734, https://doi.org/10.1002/joc.1623.

Degefu, W., 1987: Some aspects of meteorological drought in Ethiopia. *Drought and Hunger in Africa: Denying Famine a Future*, M. H. Glanz, Ed., Cambridge University Press, 23–36.

Diro, G. T., E. Black, and D. I. F. Grimes, 2008: Seasonal forecasting of Ethiopian spring rains. *Meteor. Appl.*, **15**, 73–83, https://doi.org/10.1002/met.63.

——, D. I. F. Grimes, and E. Black, 2011a: Large scale features affecting Ethiopian rainfall. *African Climate and Climate Change*, C. J. R. Williams and D. R. Kniveton, Eds., Vol. 43, Advances in Global Change Research Series, Springer, 13–50.

——, ——, and ——, 2011b: Teleconnections between Ethiopian summer rainfall and sea surface temperature: Part II. Seasonal forecasting. *Climate Dyn.*, **37**, 121–131, https://doi.org/10.1007/s00382-010-0896-x.

Eden, J. M., K. Wolter, F. E. L. Otto, and G. J. van Oldenborgh, 2016: Multi-method attribution analysis of extreme precipitation in Boulder, Colorado. *Environ. Res. Lett.*, **11**, 124009, https://doi.org/10.1088/1748-9326/11/12/124009.

Ek, M. B., K. E. Mitchell, Y. Lin, E. Rogers, P. Grunmann, V. Koren, G. Gayno, and J. D. Tarpley, 2003: Implementation of Noah land surface model advances in the National Centers for Environmental Prediction operational mesoscale Eta Model. *J. Geophys. Res.*, **108**, 8851, https://doi.org/10.1029/2002JD003296.

Endalew, G. J., 2007: Changes in the frequency and intensity of extremes over northeast Africa. KNMI Sci. Rep. WR 2007-02, 45 pp.

FEWS NET, 2015: Illustrating the extent and severity of the 2015 Ethiopia drought. FEWS Net Rep., 7 pp., http://www.fews.net/east-africa/ethiopia/special-report/december-17-2015.

——, 2017: Crisis (IPC Phase 3) expected in parts of Oromia, SNNPR, and southern pastoral areas. FEWS Net Rep., 13 pp., http://www.fews.net/sites/default/files/documents/reports/Ethiopia_OL_2016_10_final.pdf.

Flato, G., and Coauthors, 2013: Evaluation of climate models. *Climate Change 2013: The Physical Science Basis*, T. F. Stocker et al., Eds., Cambridge University Press, 741–866.

Funk, C., and Coauthors, 2005: Recent drought tendencies in Ethiopia and equatorial subtropical eastern Africa. U.S. Agency for International Development, 12 pp., http://pdf.usaid.gov/pdf_docs/PNADH997.pdf.

——, S. E. Nicholson, M. Landsfeld, D. Klotter, P. Peterson, and L. Harrison, 2015a: The centennial trends Greater Horn of Africa precipitation dataset. *Sci. Data*, **2**, 150050, https://doi.org/10.1038/sdata.2015.50.

——, S. Shukla, A. Hoell, and B. Livneh, 2015b: Assessing the contributions of East African and west Pacific warming to the 2014 boreal spring East African drought [in "Explaining Extreme Events of 2014 from a Climate Perspective"]. *Bull. Amer. Meteor. Soc.*, **96**, S77–S82, https://doi.org/10.1175/BAMS-D-15-00106.1.

——, and Coauthors, 2015c: The climate hazards infrared precipitation with stations—A new environmental record for monitoring extremes. *Sci. Data*, **2**, 150066, https://doi.org/10.1038/sdata.2015.66.

——, L. Harrison, S. Shukla, A. Hoell, D. Korecha, T. Magadzire, G. Husak, and G. Galu, 2016: Assessing the contributions of local and east Pacific warming to the 2015 droughts in Ethiopia and southern Africa [in "Explaining Extreme Events of 2015 from a Climate Perspective"]. *Bull. Amer. Meteor. Soc.*, **97**, S75–S80, https://doi.org/10.1175/BAMS-D-16-0167.1.

Gissila, T., E. Black, D. I. F. Grimes, and J. M. Slingo, 2004: Seasonal forecasting of the Ethiopian summer rains. *Int. J. Climatol.*, **24**, 1345–1358, https://doi.org/10.1002/joc.1078.

Government of Ethiopia and Humanitarian Partners, 2016: 2016 Ethiopia humanitarian requirements document. 54 pp., http://reliefweb.int/sites/reliefweb.int/files/resources/ethiopia_hrd_2016.pdf.

Hansen, J., R. Ruedy, M. Sato, and K. Lo, 2010: Global surface temperature change. *Rev. Geophys.*, **48**, RG4004, https://doi.org/10.1029/2010RG000345.

Hazeleger, W., and Coauthors, 2010: EC-Earth: A seamless Earth-system prediction approach in action. *Bull. Amer. Meteor. Soc.*, **91**, 1357–1363, https://doi.org/10.1175/2010BAMS2877.1.

Hillbruner, C., and G. Moloney, 2012: When early warning is not enough—Lessons learned from the 2011 Somalia famine. *Global Food Secur.*, **1**, 20–28, https://doi.org/10.1016/j.gfs.2012.08.001.

Hoerling, M., J. Hurrell, J. Eischeid, and A. Phillips, 2006: Detection and attribution of twentieth-century northern and

southern African rainfall change. *J. Climate*, **19**, 3989–4008, https://doi.org/10.1175/JCLI3842.1.

Huang, B., and Coauthors, 2015: Extended Reconstructed Sea Surface Temperature version 4 (ERSST.v4). Part I: Upgrades and intercomparisons. *J. Climate*, **28**, 911–930, https://doi.org/10.1175/JCLI-D-14-00006.1.

IFRC, 2017: Emergency plan of action update—Ethiopia: Drought. IFRC Rep., 15 pp., http://adore.ifrc.org/Download.aspx?FileId=156069.

IPCC, 2012: *Managing the Risks of Extreme Events and Disasters to Advance Climate Change Adaptation*, C. B. Field et al., Eds., Cambridge University Press, 582 pp., https://www.ipcc.ch/pdf/special-reports/srex/SREX_Full_Report.pdf.

Jury, M. R., and C. Funk, 2013: Climatic trends over Ethiopia: Regional signals and drivers. *Int. J. Climatol.*, **33**, 1924–1935, https://doi.org/10.1002/joc.3560.

King, A. D., G. J. van Oldenborgh, and D. J. Karoly, 2016: Climate change and El Niño increase likelihood of Indonesian heat and drought [in "Explaining Extreme Events of 2015 from a Climate Perspective"]. *Bull. Amer. Meteor. Soc.*, **97**, S113–S117, https://doi.org/10.1175/BAMS-D-16-0164.1.

Korecha, D., and A. G. Barnston, 2007: Predictability of June–September rainfall in Ethiopia. *Mon. Wea. Rev.*, **135**, 628–650, https://doi.org/10.1175/MWR3304.1.

——, and A. Sorteberg, 2013: Validation of operational seasonal rainfall forecast in Ethiopia. *Water Resour. Res.*, **49**, 7681–7697, https://doi.org/10.1002/2013WR013760.

Liebmann, B., and Coauthors, 2014: Understanding recent eastern Horn of Africa rainfall variability and change. *J. Climate*, **27**, 8630–8645, https://doi.org/10.1175/JCLI-D-13-00714.1.

Lott, F. C., N. Christdis, and P. A. Stott, 2013: Can the 2011 East African drought be attributed to climate change? *Geophys. Res. Lett.*, **40**, 1177–1181, https://doi.org/10.1002/grl.50235.

Lyon, B., and D. G. DeWitt, 2012: A recent and abrupt decline in the East African long rains. *Geophys. Res. Lett.*, **39**, L02702, https://doi.org/10.1029/2011GL050337.

Marthews, T. R., F. E. L. Otto, D. Mitchell, S. J. Dadson, and R. G. Jones, 2015: The 2014 drought in the Horn of Africa: Attribution of meteorological drivers [in "Explaining Extreme Events of 2014 from a Climate Perspective"]. *Bull. Amer. Meteor. Soc.*, **96**, S83–S88, https://doi.org/10.1175/BAMS-D-15-00115.1.

Massey, N., and Coauthors, 2015: Weather@home—Development and validation of a very large ensemble modelling system for probabilistic event attribution. *Quart. J. Roy. Meteor. Soc.*, **141**, 1528–1545, https://doi.org/10.1002/qj.2455.

McNally, A., and Coauthors, 2015: Calculating crop water requirement satisfaction in the West Africa Sahel with remotely sensed soil moisture. *J. Hydrometeor.*, **16**, 295–305, https://doi.org/10.1175/JHM-D-14-0049.1.

——, and Coauthors, 2016: FLDAS Noah land surface model L4 monthly 0.1 × 0.1 degree for eastern Africa (MERRA-2 and CHIRPS), version 1. Goddard Earth Sciences Data and Information Services Center (GES DISC), accessed 12 December 2016, https://doi.org/10.5067/XLNQ30KMZVHX.

——, and Coauthors, 2017: A land data assimilation system for sub-Saharan Africa food and water security applications. *Sci. Data*, **4**, 170012, https://doi.org/10/1038/sdata.2017.12.

Peterson, T. C., and R. S. Vose, 1997: An overview of the Global Historical Climatological Network temperature database. *Bull. Amer. Meteor. Soc.*, **78**, 2837–2849, https://doi.org/10.1175/1520-0477(1997)078<2837:AOOTGH>2.0.CO;2.

Polson, D., M. Bollasina, G. C. Hegerl, and L. J. Wilcox, 2014: Decreased monsoon precipitation in the Northern Hemisphere due to anthropogenic aerosols. *Geophys. Res. Lett.*, **41**, 6023–6029, https://doi.org/10.1002/2014GL060811.

Rowell, D. P., B. B. B. Booth, S. E. Nicholson, and P. Good, 2015: Reconciling past and future rainfall trends over East Africa. *J. Climate*, **28**, 9768–9788, https://doi.org/10.1175/JCLI-D-15-0140.1.

Schaller, N., F. E. L. Otto, G. J. van Oldenborgh, N. R. Massey, S. Sparrow, and M. R. Allen, 2014: The heavy precipitation event of May–June 2013 in the upper Danube and Elbe basins [in "Explaining Extreme Events of 2013 from a Climate Perspective"]. *Bull. Amer. Meteor. Soc.*, **95**, S69–S72, https://doi.org/10.1175/1520-0477-95.9.S1.1.

Schüttemeyer, D., A. F. Moene, A. A. M. Holtslag, and H. A. R. de Bruin, 2008: Evaluation of two land surface schemes used in terrains of increasing aridity in West Africa. *J. Hydrometeor.*, **9**, 173–193, https://doi.org/10.1175/2007JHM797.1.

Segele, Z. T., and P. J. Lamb, 2005: Characterization and variability of Kiremt rainy season over Ethiopia. *Meteor. Atmos. Phys.*, **89**, 153–180, https://doi.org/10.1007/s00703-005-0127-x.

Shongwe, M. E., G. J. van Oldenborgh, B. van den Hurk, and M. van Aalst, 2011: Projected changes in mean and extreme precipitation in Africa under global warming. Part II: East Africa. *J. Climate*, **24**, 3718–3733, https://doi.org/10.1175/2010JCLI2883.1.

Singh, R., and Coauthors, 2016: Reality of resilience: Perspectives of the 2015–16 drought in Ethiopia. *BRACED Resilience Intel*, No. 6, http://www.braced.org/resources/i/?id=18256c98-2a10-4586-9317-17a68b45c1a7.

Sippel, S., F. E. L. Otto, M. Flach, and G. J. van Oldenborgh, 2016: The role of anthropogenic warming in 2015 central European heat waves [in "Explaining Extreme Events of 2015 from a Climate Perspective"]. *Bull. Amer. Meteor. Soc.*, **97**, S51–S56, https://doi.org/10.1175/BAMS-D-16-0150.1.

Stark, J. D., C. J. Donlon, M. J. Martin, and M. E. McCulloch, 2007: OSTIA: An operational, high-resolution, real time, global sea surface temperature analysis system. *Proc. OCEANS 2007—Europe*, Aberdeen, Scotland, United Kingdom, IEEE, 061214-029, https://doi.org/10.1109/OCEANSE.2007.4302251.

Stone, D. A., and M. R. Allen, 2005: The end-to-end attribution problem: From emissions to impacts. *Climatic Change*, **71**, 303–318, https://doi.org/10.1007/s10584-005-6778-2.

Taylor, K. E., R. J. Stouffer, and G. A. Meehl, 2012: An overview of CMIP5 and the experiment design. *Bull. Amer. Meteor. Soc.*, **93**, 485–498, https://doi.org/10.1175/BAMS-D-11-00094.1.

Teuling, A. J., and Coauthors, 2013: Evapotranspiration amplifies European summer drought. *Geophys. Res. Lett.*, **40**, 2071–2075, https://doi.org/10.1002/grl.50495.

Uhe, P., F. E. L. Otto, K. Haustein, G. J. van Oldenborgh, A. D. King, D. C. H. Wallom, M. R. Allen, and H. Cullen, 2016: Comparison of methods: Attributing the 2014 record European temperatures to human influences. *Geophys. Res. Lett*, **43**, 8685–8693, https://doi.org/10.1002/2016GL069568.

van der Wiel, K., and Coauthors, 2017: Rapid attribution of the August 2016 flood-inducing extreme precipitation in south Louisiana to climate change. *Hydrol. Earth Syst. Sci.*, **21**, 897–921, https://doi.org/10.5194/hess-21-897-2017.

van Loon, A. F., and Coauthors, 2016: Drought in the Anthropocene. *Nat. Geosci.*, **9**, 89–91, https://doi.org/10.1038/ngeo2646.

van Oldenborgh, G. J., R. Haarsma, H. De Vries, and M. R. Allen, 2015: Cold extremes in North America vs. mild weather in Europe: The winter of 2013–14 in the context of a warming world. *Bull. Amer. Meteor. Soc.*, **96**, 707–714, https://doi.org/10.1175/BAMS-D-14-00036.1.

——, and Coauthors, 2016: Rapid attribution of the May/June 2016 flood-inducing precipitation in France and Germany to climate change. *Hydrol. Earth Syst. Sci. Discuss.*, 1–23, https://doi.org/10.5194/hess-2016-308.

Viste, E., D. Korecha, and A. Sorteberg, 2013: Recent drought and precipitation tendencies in Ethiopia. *Theor. Appl. Climatol.*, **112**, 535–551, https://doi.org/10.1007/s00704-012-0746-3.

Williams, A. P., and C. Funk, 2011: A westward extension of the warm pool leads to a westward extension of the Walker circulation, drying eastern Africa. *Climate Dyn.*, **37**, 2417–2435, https://doi.org/10.1007/s00382-010-0984-y.

Yilmaz, M. T., M. C. Anderson, B. Zaitchik, C. R. Hain, W. T. Crow, M. Ozdogan, J. A. Chun, and J. Evans, 2014: Comparison of prognostic and diagnostic surface flux modeling approaches over the Nile River basin. *Water Resour. Res.*, **50**, 386–408, https://doi.org/10.1002/2013WR014194.